Check for updates

Batteries & Supercaps

Review
doi.org/10.1002/batt.202500655

Chemistry Europe
European Chemical Societies Publishing

www.batteries-supercaps.org

Electrospun Nanofiber Architectures for High-Performance Aqueous Zinc Ion Batteries

Yulu Huo, Yurong Fan, Xu Liu, Zhiwu Wang, Nien-Chu Lai, Cunhai Wang,* Nü Wang,* Yong Zhao, and Jingchong Liu*

Aqueous zinc ion batteries (AZIBs) are regarded as promising candidates for large-scale energy storage due to their intrinsic safety, environmental friendliness, and high energy density. However, their practical deployment is hindered by several challenges, including dendrite growth on the anode, dissolution and structural degradation of cathode materials, and the limitations of conventional separators. To address these issues, various materials have been explored. Among them, electrospun nanofibers have emerged as a particularly attractive solution owing to their controllable nanostructures, large specific surface area, and tunable porosity. Although the application of electrospun nanofibers in AZIBs has expanded rapidly in recent years, a systematic review focusing on this topic remains lacking. To fill this gap, this review comprehensively summarizes the recent progress in leveraging electrospun nanofibers to overcome key limitations in AZIBs. Beginning with the fundamentals and structural design strategies of electrospinning, it highlights advances in their integration into cathodes, anode, and separators. Special emphasis is placed on elucidating the working mechanisms of the nanofibers and the structure–performance correlations between their microstructure and electrochemical properties. Finally, the review outlines future directions and remaining challenges in this field, aiming to offer valuable insights for the rational design of electrospun nanofiber architectures toward more efficient AZIBs.

1. Introduction

The escalating demand for sustainable energy has spurred an urgent need for reliable and safe energy storage systems.[1–3] Lithium-ion batteries are the most widely deployed technology in this field because of their relative high energy density,[4] with extensive applications spanning portable electronics, electric vehicles, and grid-scale energy storage. Yet long-term deployment has revealed inherent challenges, including high production costs that hinder large-scale adoption,[5] environmental burdens from toxic components in end-of-life batteries,[6] and safety risks from thermal runaway under conditions of overcharging, deep discharging or mechanical damage.[7–9] These limitations highlight the need for alternative energy storage technologies capable of meeting safety, cost, and sustainability requirements.

Aqueous zinc ion batteries (AZIBs) have thus garnered significant attention as promising candidates for stationary grid storage.[10–13] Their advantages include the intrinsic safety of nonflammable aqueous electrolytes with high specific heat capacity, relatively low cost, and environmentally benign chemistry.[14–16] Despite these advantages, several fundamental challenges still hinder practical implementation, such as dendrite growth at anodes that may induce short-circuit failures[17] and structural degradation of cathode materials that accelerates capacity fading and limits cycle life.[18–23] In addition, conventional separators such as glass fiber, filter paper, and nonwoven mats often fail to deliver the necessary combination of mechanical robustness, electrolyte wettability, ionic conductivity, and electrical insulation.[24,25] further constraining the durability and energy density of AZIBs in large-scale applications. These challenges have motivated intensive efforts to develop functional materials and advanced fabrication strategies that can stabilize electrode interfaces, optimize ion transport and extend the operating lifetime of AZIBs.

To address these challenges, novel material fabrication technologies and functional materials have been extensively explored.[26–30] Among these, electrospinning stands out for its capability to fabricate continuous nano/microscaled fibers with precise structural control, offering a promising pathway to overcome the performance bottlenecks of AZIBs.[31,32] The resulting electrospun nanofibers possess advantageous features such as large specific surface area, high aspect ratios, tunable alignment for directed transport, and shortened ion diffusion pathways,[33–36] which are critical for enhancing electrochemical performance and cycling stability. These attributes render electrospun nanofibers particularly effective

Y. Huo, X. Liu, Z. Wang, J. Liu
School of Chemistry and Biological Engineering
University of Science and Technology Beijing
Beijing 100083, China
E-mail: jchliu@ustb.edu.cn

Y. Fan
School of Aeronautic Science and Engineering
Beihang University
Beijing 100191, China

N.-C. Lai, C. Wang
School of Energy and Environmental Engineering
University of Science and Technology Beijing
Beijing 100083, China
E-mail: wangcunhai@ustb.edu.cn

N. Wang, Y. Zhao
School of Chemistry
Beihang University
Beijing 100191, China
E-mail: wangn@buaa.edu.cn

© 2025 Wiley-VCH GmbH

when deployed as anode, cathode, and separators in AZIBs. As illustrated in **Figure 1**, electrospinning enables the design of diverse nanofiber architectures—including composite, hierarchical hollow, spongy-like, pearl-necklace, metal–organic frameworks (MOFs)-based, core–shell, bimetallic, hybrid, surface-modified, and pure nanofibers—that can be tailored for specific roles within AZIBs. These nanofibers can serve as advanced electrode materials offering improved conductivity and stability, or as highly efficient separators with enhanced electrolyte affinity and mechanical integrity. Such structural versatility allows for the optimization of ion transport kinetics, suppression of dendrite formation, and enhancement of cycling performance, positioning electrospun nanofibers as key enablers in the development of next-generation AZIBs systems. **Figure 2** summarizes a concise timeline of representative electrospinning-enabled advancements in aqueous batteries. Since 2010, the application of electrospinning in aqueous batteries has attracted growing interest. Early work demonstrated its potential through the use of flexible carbon nanofibers (CNFs) as a cathode support material, highlighting the ability of fibrous architectures to enhance electrochemical performance (Figure 2a).[37] In 2018, polyaniline (PANI)-coated CNFs were used as a cathode material (Figure 2b),[38] expanding the application of electrospun fibers toward conductive polymer-based electrodes. By 2020, a polybenzimidazole (PBI) nanofiber layer fabricated via electrospinning was applied as a protective coating for zinc (Zn) anodes (Figure 2c),[39] effectively suppressing the growth of Zn dendrites. In the same year, vanadium pentoxide (V_2O_5) nanofibers with intentional physical and chemical defects were produced through electrospinning (Figure 2d).[40] Their distinctive architecture and defect-mediated synergy significantly improved Zn^{2+} storage capabilities. In 2021, electrospinning was also utilized to fabricate a heat-resistant nanofiber membrane separator suitable for aqueous lithium-ion batteries (Figure 2e),[41–43] underscoring the versatility of the technique. Concurrently, nickel-cobalt sulfide-embedded CNFs ($NiCo_2S_4$@CNFs) were prepared as lightweight, flexible, and binder-free cathodes, exhibiting remarkable electrochemical performance (Figure 2f).[44] In 2022, an electrospun polyacrylonitrile (PAN) nanofibrous separator was designed to modulate Zn deposition behavior, thereby enhancing cycling stability (Figure 2g).[29] The following year, a vanadium dioxide/CNFs (VO_2/CNFs) was produced via electrospinning and employed as a cathode in AZIBs, delivering high specific capacity and excellent cycling endurance (Figure 2h).[45] In 2024, a composite of V_2O_5 embedded within CNFs was prepared using electrospinning. Its improved ionic conductivity and structural stability offered new insights into the design of aqueous Zn-ion batteries.[46] Furthermore, in 2025, an electrospun titanium dioxide/CNFs (TiO_2/CNFs) interlayer separator was developed for aqueous Zn-ion batteries (Figure 2j),[47] markedly improving cycle life and operational stability. Simultaneously, electrospinning was also applied to aqueous ammonium-ion batteries, where sulfur-doped CNFs coupled with $Ti_3C_2T_x$ were constructed, leading to a substantial increase in ammonium-ion adsorption capacity (Figure 2k).[48]

Although the application of electrospun nanofibers in AZIBs has expanded rapidly, a systematic review dedicated to this topic is still lacking. It is therefore imperative to consolidate recent progress in electrospinning-derived nanomaterials for AZIBs systems. This review aims to systematically delineate research advances in electrospun nanofibers for AZIBs. First, we outline the fundamental principles of electrospinning, including process parameters and the influence of ambient conditions on fiber formation. We then examine their applications in AZIBs with a focus on anodes, cathodes, and separators, highlighting the relationship between structural design and electrochemical performance. Finally, we discuss the persisting challenges, potential directions for future research, and the opportunities offered by electrospinning to advance AZIBs

Cunhai Wang is an associate professor at University of Science and Technology Beijing (USTB), Beijing, China. Before joining USTB at 2018, Dr. Wang carried out scientific research at Harbin Institute of Technology where he received his PhD in engineering (2018). He was a visiting scholar at University of California, Berkeley from Sept. 2015 to Oct. 2016. Dr. Wang has been devoting himself to energy conversion and management, including radiative cooling, solar utilization, and microstructures for energy harvesting. Dr. Wang is now focusing on alleviating global energy issues by developing and promoting space thermal radiation-driven sustainable technologies.

Nü Wang is a Professor at Beihang University (BUAA), Beijing, China. Prof. Wang's research focuses on the preparation and structural analysis of bio-inspired functional micro/nanofibers, as well as the electrospinning fabrication and property investigation of organic/inorganic hierarchical micro/nanofibrous materials.

Jingchong Liu is an associate professor at University of Science and Technology Beijing (USTB), Beijing, China. His research focuses on the development of bioinspired smart films for the controllable transport of mass and heat. By precisely regulating the transport behavior of photons, ions, and molecules, his work aims to contribute to energy conservation and emission reduction. Dr. Liu's current research explores innovative applications of bioinspired smart thin films in the environmental field, energy systems, sustainable agriculture, and mass and heat transfer management in space systems.

© 2025 Wiley-VCH GmbH

25666223, 0, Downloaded from https://chemistry-europe.onlinelibrary.wiley.com/doi/10.1002/batt.202500655 by University of Ulsan, Wiley Online Library on [11/11/2025]. See the Terms and Conditions (https://onlinelibrary.wiley.com/terms-and-conditions) on Wiley Online Library for rules of use; OA articles are governed by the applicable Creative Commons License

Review
doi.org/10.1002/batt.202500655
Chemistry Europe
European Chemical Societies Publishing

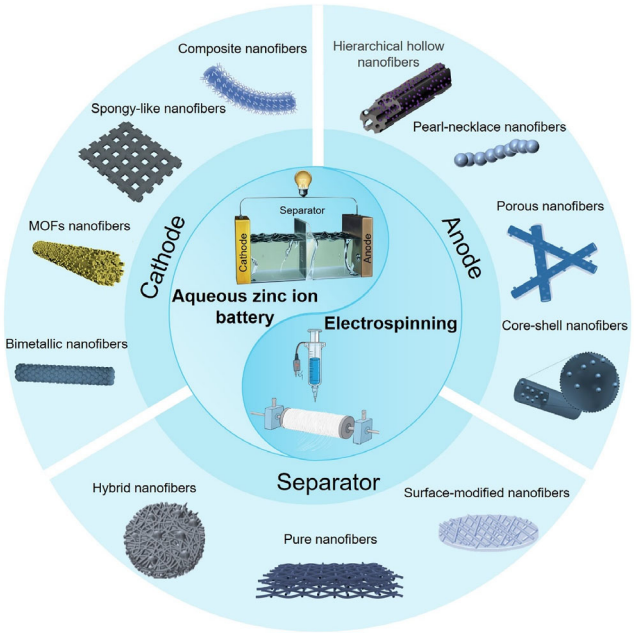

Figure 1. Schematic illustration of electrospun nanofiber architectures and their applications in AZIBs. Electrospinning technology facilitates the fabrication of various nanofiber morphologies—such as composite, hierarchical hollow, spongy-like, pearl-necklace, MOFs-based, core–shell, bimetallic, hybrid, surface-modified, and pure nanofibers—which can be strategically incorporated into cathodes, anodes, and separators.

technologies. This review is expected to serve as a resource for understanding the current state of electrospinning in AZIBs, to guide the rational design of nanofiber-based materials, and to inspire further research into safe, cost-effective and high-performance energy storage systems.

2. Principles and Processing Technology of Electrospinning

Electrospinning, a technique first patented in 1934, enables the direct and continuous production of polymer nanofibers.[49,50] The basic principle involves dissolving polymer precursors in a solvent to generate nanofibers under an electric field, while the scope of electrospinning has been extended beyond polymers to include metals, ceramics, semiconductors, proteins, and hybrid systems.[51] Owing to their large specific surface area, high porosity, unique nanostructures, and hybrid characteristics, electrospun nanofibers offer broad opportunities in energy storage.[52,53]

A conventional electrospinning apparatus consists of a high-voltage power supply, a syringe containing the precursor solution or melt, and a grounded collector.[54] Upon application of voltage exceeding a critical threshold between the nozzle and collector, a Taylor cone forms at the nozzle tip and a charged jet is ejected.[55] After initial elongation, the jet undergoes bending instability and is progressively stretched, accompanied by solvent evaporation and phase separation, ultimately solidifying as nanofibers on the collector.[56]

The architecture and morphology of electrospun nanofibers are dictated by multifactorial parameters spanning polymer solution properties, processing variables, and environmental conditions. Critical determinants include: 1) solution parameters (precursor type, concentration, viscosity),[49,55,57,58] 2) operational parameters (applied voltage,[59] flow rate,[60] nozzle-collector distance[61,62] temperature/humidity),[63,64] and 3) post-treatment methodologies. Precise orchestration of these factors integrated with postprocessing (e.g., thermal annealing) enables fabrication of sophisticated nanostructures with tunable hierarchical features, exemplified by nonwoven aligned fibers, nanoribbons, nanorods, and stochastic 3D assemblies.[65]

Electrospinning therefore offers a scalable and adaptable route for constructing nanofibrous architectures with controlled morphology and composition. Such structures provide a favorable platform for regulating electrode–electrolyte interfaces and ion transport dynamics, laying the foundation for their integration into AZIBs. Building on these advantages, the following section discusses how electrospun nanofibers have been applied across different components of AZIBs.

3. Applications of Electrospun Nanofibers in AZIBs

Electrospun nanofibers have gained widespread application in AZIBs due to their versatility and adaptability. Their mechanical flexibility supports the development of robust and durable cell components, while the interconnected fibrous networks reduce ion transport distances and interfacial resistance compared with conventional separators. Moreover, conductive and stable nanofibers can be incorporated into anodes to regulate Zn deposition and suppress dendrite formation. In addition, separators fabricated by electrospinning can be precisely tailored in thickness, pore size, and mechanical strength, providing enhanced electrolyte wettability, efficient ion transport, and effective resistance against dendrite penetration. With these advantages, electrospun nanofibers have been explored in cathodes, anodes, and separators for AZIBs, as detailed in the following subsections.

3.1. Cathodes

The cathode, as the core component of AZIBs, largely determines the electrochemical performance of the cell.[66,67] Consequently, the development of high-performance cathode materials has been a major research focus over the past decade.[68] However, these materials still face limitations such as poor electrical conductivity, dissolution in aqueous electrolytes, and volume expansion during cycling.[69] Electrospun CNFs offer a promising strategy to address these issues by constructing highly conductive carbon-based frameworks, which significantly enhance the overall electrical conductivity and reaction kinetics of the electrode.[70] Their porous structure and large surface area further enable the integration of active species, which helps alleviate dissolution and buffer volume changes.[71] For a clear and structured elaboration, the following

© 2025 Wiley-VCH GmbH

25666223, 0, Downloaded from https://chemistry-europe.onlinelibrary.wiley.com/doi/10.1002/batt.202500655 by University of Ulsan, Wiley Online Library on [11/11/2025]. See the Terms and Conditions (https://onlinelibrary.wiley.com/terms-and-conditions) on Wiley Online Library for rules of use; OA articles are governed by the applicable Creative Commons License

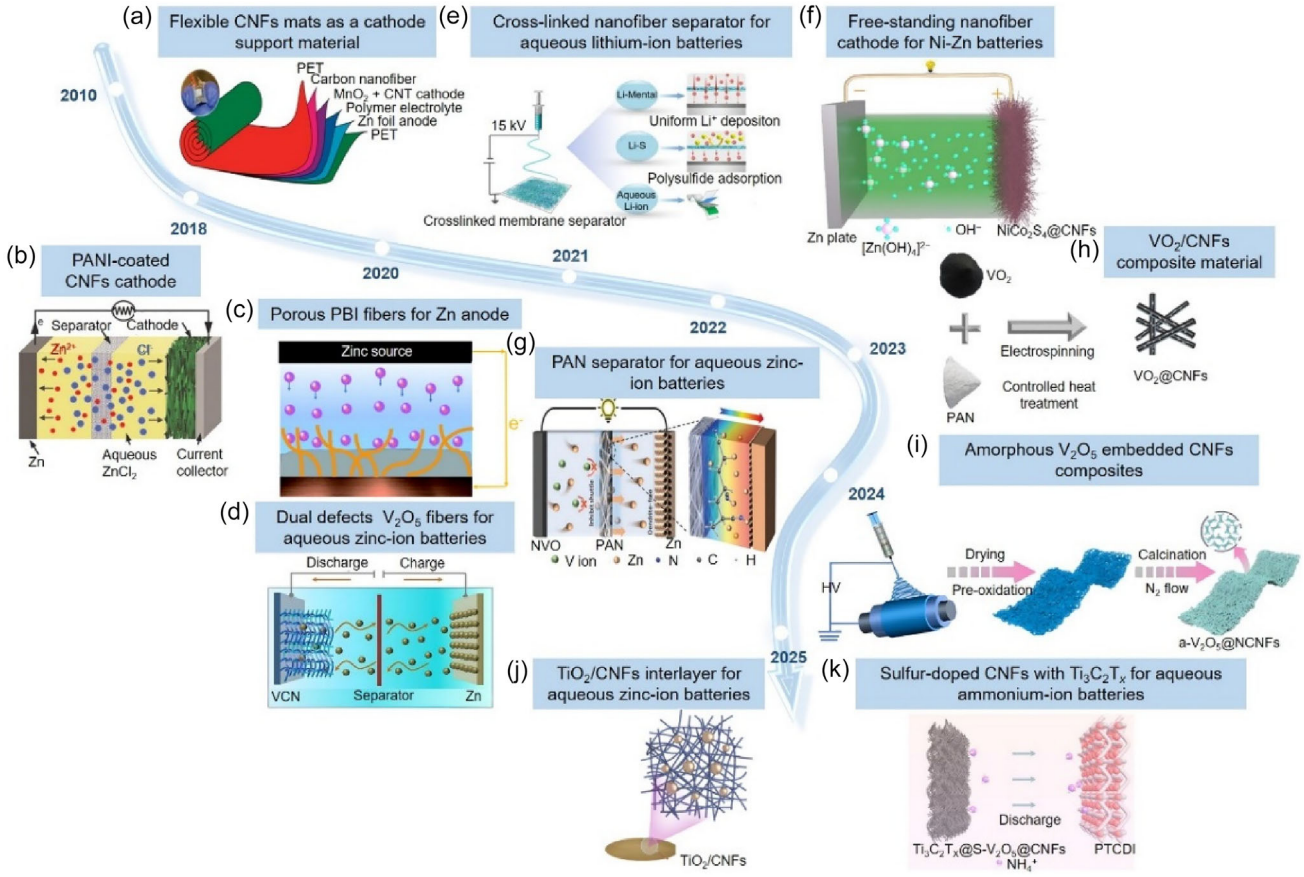

Figure 2. Timeline of representative electrospinning-enabled advancements in AZIBs. Copyright permissions obtained for figures. a) Electrospun CNFs as a cathode support material (2010).[37] b) PANI-coated CNFs applied as cathode materials (2018).[38] c) PBI nanofiber layer fabricated as a protective coating for Zn anodes (2020).[39] d) V_2O_5 nanofibers with defect engineering for enhanced Zn^{2+} storage (2020).[40] e) Heat-resistant nanofiber membrane separator designed for aqueous lithium-ion batteries (2021).[41] f) $NiCo_2S_4$ embedded in CNFs used as flexible binder-free cathodes (2021).[44] g) PAN nanofibrous separator regulating Zn deposition and cycling stability (2022).[29] h) VO_2/CNFs applied as cathodes for Zn-ion batteries (2023).[45] i) V_2O_5 embedded in CNFs for improved conductivity and structural stability (2024).[46] j) TiO_2/CNF interlayers used as separators for Zn-ion batteries (2025).[47] k) Sulfur-doped CNFs coupled with $Ti_3C_2T_x$ employed in ammonium-ion batteries to enhance ion adsorption (2025).[48]

sections will detail the application of electrospun nanofibers in cathodes, covering vanadium (V)-based materials, manganese (Mn)-based materials, iodine (I)-based cathodes, nickel (Ni)-based cathodes, and other cathode materials.

3.1.1. V-Based Cathodes

V-based oxides represent one of the most promising cathode materials for AZIBs due to their multiple oxidation states, high theoretical specific capacity, and rich crystal chemistry.[72,73] However, they are prone to dissolution in mildly acidic electrolytes, which leads to capacity fading and unwanted deposition on the Zn anode surface.[74] In addition, V-based materials are typically semiconductors with poor intrinsic electronic conductivity, necessitating the incorporation of conductive additives during electrode fabrication.[75] Electrospinning provides an effective route to improve these properties by enabling nanostructuring and compositing strategies. For instance, Volkov et al.[76] synthesized V_2O_5 nanofibers via sol–gel processing followed by thermal treatment (**Figure 3**a). This nanofibrous architecture provided a high specific surface area and favorable ion transport pathways. When employed as the cathode active material (70 wt%), the V_2O_5 nanofiber electrode delivered enhanced electrochemical performance, exhibiting 101% capacity retention after 500 cycles at 0.2 A g^{-1} (Figure 3b). This demonstrates the efficacy of electrospun V_2O_5 nanofibers in enhancing capacity, rate capability, and mitigating dissolution. Heteroatom doping is an effective strategy for tailoring the intrinsic electronic/ionic properties of electrode materials for AZIBs.[77] Doping atoms can expand the interlayer spacing and redistribute the charge density of surface atoms, thereby increasing ion storage sites and facilitating electron transport.[78,79] Wang et al.[46] fabricated amorphous V_2O_5 embedded within nitrogen-doped CNFs (a-V_2O_5@NCNFs) via electrospinning. This design achieved a triple synergistic effect through uniform carbon coating. TEM images show that nanoparticles are evenly encapsulated in CNFs (Figure 3c). The composite cathode exhibited good cycling stability at a moderate current density (1 A g^{-1}), delivering an initial discharge capacity of 281 mAh g^{-1} with >96% retention after 100 cycles (Figure 3d). Remarkably, it maintained 87.3% capacity retention after 5,000 cycles at 5 A g^{-1}, outperforming conventional physically mixed

© 2025 Wiley-VCH GmbH

25666223, 0, Downloaded from https://chemistry-europe.onlinelibrary.wiley.com/doi/10.1002/batt.202500655 by University of Ulsan, Wiley Online Library on [11/11/2025]. See the Terms and Conditions (https://onlinelibrary.wiley.com/terms-and-conditions) on Wiley Online Library for rules of use; OA articles are governed by the applicable Creative Commons License

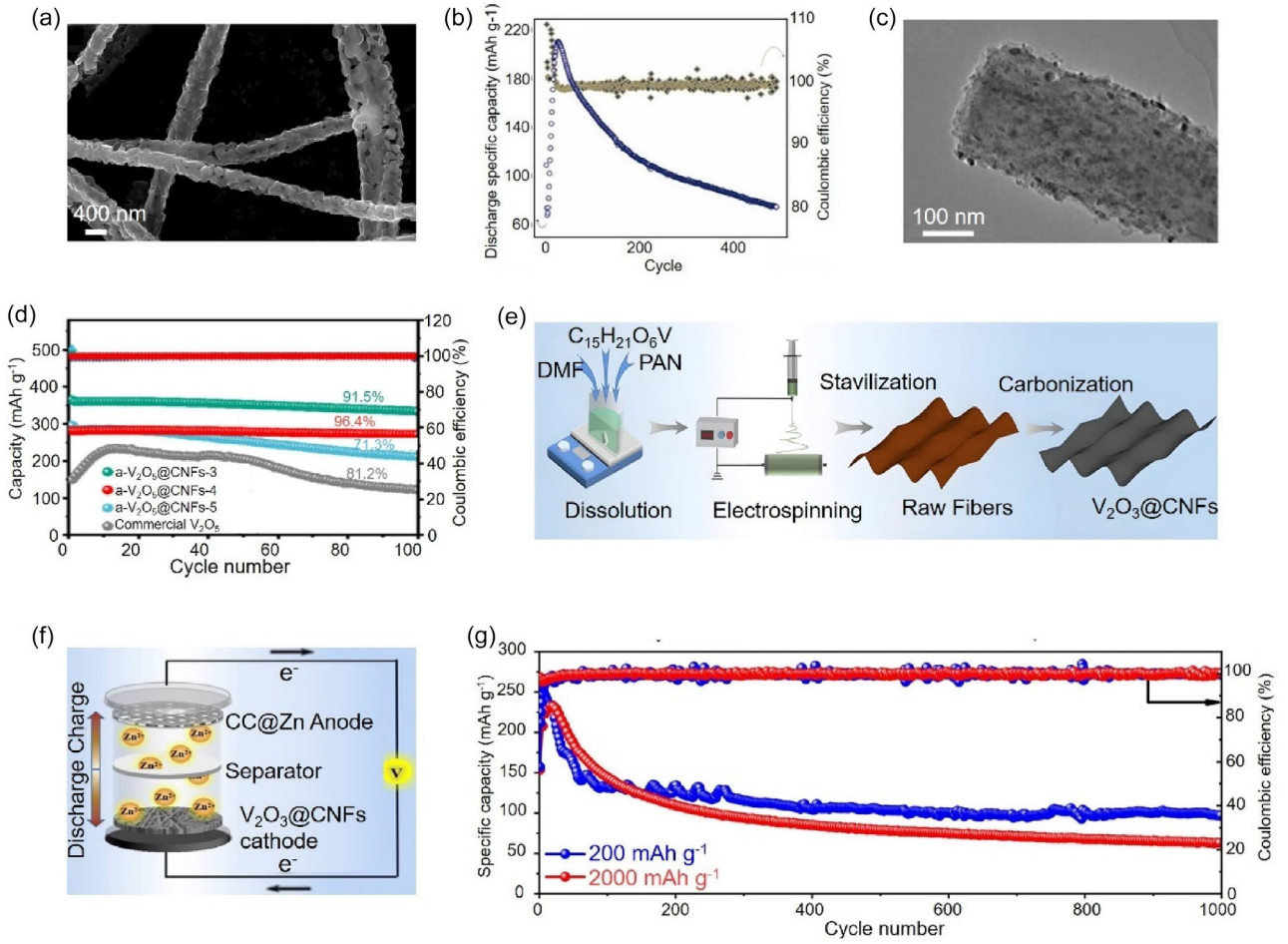

Figure 3. Electrospun nanofibers-enabled V_2O_5 and V_2O_3-based cathodes for AZIBs. Copyright permissions obtained for figures. a) SEM images of V_2O_5 nanofibers.[76] b) Cycling performance of V_2O_5 nanofibers at 0.2 A g^{-1}.[76] c) TEM images of a-V_2O_5@NCNFs.[46] d) Cycling performance of a-V_2O_5@NCNFs at 1 A g^{-1} for 100 cycles.[46] e) Schematic illustration of the fabrication of V_2O_3@CNFs.[81] f) Schematic illustration of the V_2O_3@CNFs//Zn@CC full battery.[81] g) Long cycling performance and CE of the V_2O_3@CNFs electrode.[81]

V/carbon composites. Liu et al.[80] embedded V_2O_5 nanodots within CNFs via electrospinning to create a binder-free, self-supporting cathode. This structure effectively suppressed V dissolution and eliminated the need for additives. It achieved a capacity of 215 mAh g^{-1} at a high current density of 20 A g^{-1} and retained 63% capacity after 18,000 cycles. Liu et al.[81] prepared a flexible, self-supporting V_2O_3@N-doped CNFs electrode (Figure 3e). The uniform dispersion of V_2O_3 nanoparticles within the CNFs, combined with a 3D tunnel structure, accelerated Zn^{2+} transport (Figure 3f), resulting in a stable capacity of 65 mAh g^{-1} after 1,000 cycles at 2,000 mA g^{-1} (Figure 3g) and demonstrated a threefold improvement in rate performance. Zhang et al.[82] combined V-based MOFs (V-MOFs) with electrospinning to construct hierarchically structured Vanadium nitride (VN)/N-CNFs (**Figure 4**a). VN nanocrystals were embedded within the CNFs backbone and branches (Figure 4b). Upon electrochemical activation, this material transformed into a $V_2O_5{\cdot}nH_2O$ phase, delivering a high capacity of 297 mAh g^{-1} at an ultrahigh rate of 100 A g^{-1}. It also demonstrated exceptional stability over 30,000 cycles at 50 A g^{-1} (specific capacity: 482 mAh g^{-1}). Wang et al.[83] further employed an MOF-derived strategy, combining electrospinning with a pore-forming agent to prepare VN-decorated N-doped micro/mesoporous CNFs (VN/N-MCNFs). The precisely engineered pore channels (>3.35 nm) matched the solvated $[Zn(H_2O)_6]^{2+}$ structure (>0.86 nm), significantly enhancing Zn^{2+} accessibility. This resulted in a high capacity retention of 86.1% after 5,000 cycles at 5 A g^{-1}, far exceeding that of a nonporous control. In these composite electrodes, the conductive carbon matrix plays a dual role by mitigating V dissolution and reducing the reliance on binders or conductive additives, which contributes to achieving high discharge capacity and energy density.[84]

In recent years, defect engineering has emerged as a promising strategy for enhancing the electrochemical performance of cathode materials.[85,86] Physical defects within the host material, such as micropores or cracks, can shorten ion diffusion distances and improve electrolyte accessibility.[87] Furthermore, introducing chemical defects into transition metal oxides has proven effective for modulating their electronic and/or crystal structures.[88–91] The rich V–O phase diagram facilitates the creation of complex chemical defects—such as cation or oxygen vacancies—within diverse crystal structures, which promote Zn^{2+} insertion/extraction

© 2025 Wiley-VCH GmbH

25666223, 0, Downloaded from https://chemistry-europe.onlinelibrary.wiley.com/doi/10.1002/batt.202500655 by University of Ulsan, Wiley Online Library on [11/11/2025]. See the Terms and Conditions (https://onlinelibrary.wiley.com/terms-and-conditions) on Wiley Online Library for rules of use; OA articles are governed by the applicable Creative Commons License

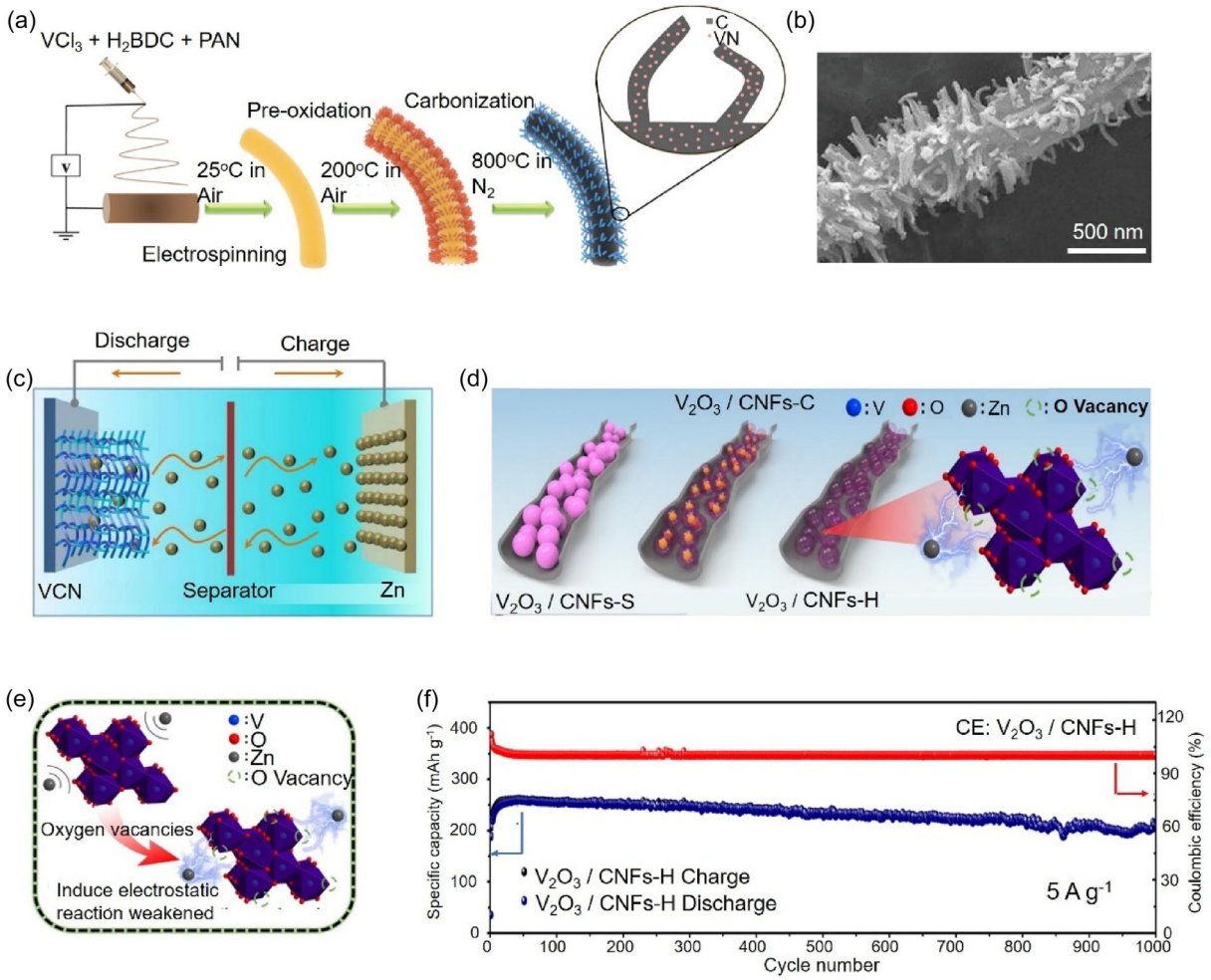

Figure 4. Electrospun nanofibers-enabled VN and defect-engineered V-based cathodes for AZIBs. Copyright permissions obtained for figures. a) Schematic illustration of the synthesis procedures for 3D self-supported hierarchical VN/N-CNFs skeleton.[82] b) SEM images of VN/N-CNFs.[82] c) Schematic diagram of the VCN//Zn full battery.[40] d) Schematic illustration of synthesis process for V_2O_3/CNFs-soild, V_2O_3/CNFs-core–shell, and V_2O_3/CNFs-hollow composites.[94] e) Structural schematic diagram of oxygen vacancies weaken electrostatic reaction.[94] f) The long cycling performance of V_2O_3/CNFs-H at 5 A g^{-1}.[94]

kinetics.[92,93] Chen et al.[40] employed electrospinning to fabricate VCN incorporating both physical and chemical defects (Figure 4c). VCN exhibits a high capacity (256 mAh g^{-1} at 1 A g^{-1}) and excellent cycle stability (with only a 17% capacity fade after 1000 cycles at 5 A g^{-1}). Song et al.[94] embedded V_2O_3 nanospheres of tailored morphologies involving solid, core–shell, hollow into N-doped CNFs (solid, core–shell, hollow) via electrospinning combined with thermal treatment (Figure 4d). These tailored V_2O_3 nanostructures possess abundant oxygen vacancies, which mitigate volume expansion effects and provide additional pathways for Zn^{2+} transport (Figure 4e). The V_2O_3/CNFs-hollow electrode demonstrated exceptional stability, retaining a reversible capacity of 202 mAh g^{-1} after 1,000 cycles at 5 A g^{-1} with negligible capacity decay (Figure 4f). Therefore, electrospinning provides effective structural and compositional regulation to overcome the inherent drawbacks of V-based cathodes, including poor conductivity, dissolution, and volume variation. Approaches such as carbon compositing, heteroatom doping, and defect engineering have enhanced ion transport, cycling stability, and rate capability. Despite these advances, challenges remain in mitigating dissolution during extended cycling, achieving scalable and reproducible fabrication, and clarifying the mechanisms of ion insertion and phase evolution. Progress in these areas will be crucial for advancing electrospun V-based cathodes toward practical aqueous energy storage systems.

While electrospun V-based cathodes show considerable potential, obstacles must be overcome before commercialization. Vanadium dissolution remains a primary concern, leading to progressive capacity fade, particularly under high-rate or prolonged cycling conditions. Scaling up electrospinning to fabricate defect-free fibers with homogeneous dopant incorporation continues to pose substantial manufacturing challenges. A deeper mechanistic understanding of Zn^{2+} insertion processes and structural evolution in defective or multi-electron reaction environments is also urgently needed. Future studies should prioritize the development of functional electrolytes or interface-stabilizing coatings to inhibit dissolution, alongside advanced in situ diagnostics and modeling to unravel complex reaction pathways. Overcoming these limitations is vital for deploying V-based cathodes in high-performance AZIBs.

© 2025 Wiley-VCH GmbH

25666223, 0, Downloaded from https://chemistry-europe.onlinelibrary.wiley.com/doi/10.1002/batt.202500655 by University of Ulsan, Wiley Online Library on [11/11/2025]. See the Terms and Conditions (https://onlinelibrary.wiley.com/terms-and-conditions) on Wiley Online Library for rules of use; OA articles are governed by the applicable Creative Commons License

25666223, 0, Downloaded from https://chemistry-europe.onlinelibrary.wiley.com/doi/10.1002/batt.202500655 by University of Ulsan, Wiley Online Library on [11/11/2025]. See the Terms and Conditions (https://onlinelibrary.wiley.com/terms-and-conditions) on Wiley Online Library for rules of use; OA articles are governed by the applicable Creative Commons License

3.1.2. Mn-Based Cathodes

Mn-based materials (including MnO, MnO_2, Mn_2O_3, Mn_3O_4) have been extensively investigated for rechargeable AZIBs owing to their high operating voltage, low cost, natural abundance, and nontoxicity.[95–99] Conventional electrodes are typically fabricated by mixing Mn-based oxides powders with conductive additives, binders, and current collectors. This configuration, together with the intrinsically low electronic conductivity of Mn-based oxides and their tendency to aggregate, restricts fast-charging capability at high current densities.[100]

Among these materials, MnO is attractive due to its low cost, environmental benignity, and structural stability during cycling.[101] It has found widespread application in energy storage devices such as lithium-ion batteries and supercapacitors.[102–106] However, the achievable specific discharge capacity of pristine MnO in AZIBs remains unsatisfactory, primarily due to sluggish reaction kinetics. Electrospinning offers a means to incorporate MnO into conductive 1D CNFs, which provide improved charge transport and directional electron migration compared with conventional carbon matrices.[107] Nevertheless, achieving highly uniform and dense MnO–carbon composites remains challenging, and the poor intrinsic conductivity of MnO further constrains performance.[108] To address these limitations, recent work has explored electrospinning strategies to construct integrated MnO–carbon architectures with improved conductivity and structural uniformity. Chen et al.[109] fabricated oxygen vacancy-rich MnO_{1-x} embedded within CNFs (MnO_{1-x}/CNFs) via electrospinning. The introduced oxygen vacancies not only enhance intrinsic electronic conductivity but also serve as active sites facilitating Zn^{2+} adsorption and diffusion, thereby improving reaction kinetics. The CNFs provide a lightweight conductive network, enabling the cathode to deliver a high specific capacity of 264 mAh g^{-1} at 0.1 A g^{-1} and maintain exceptional capacity retention of 90% after 2,500 cycles at 2 A g^{-1}. He et al.[110] developed in situ electrospun MnO@CNFs composites as cathodes for rechargeable AZIBs (**Figure 5**a). The continuous 1D carbon nanofiber network offers long-range electron transport pathways, while its mesoporous architecture shortens ion diffusion distances and facilitates electrolyte permeability, synergistically enhancing electrochemical activity. Figure 5b shows the TEM images of the MnO@CNFs composites. This material features a robust conductive network and mesoporous architecture, significantly enhancing electrochemical activity. Uniform and intimate encapsulation of all MnO nanoparticles within the 1D CNFs imparts structural stability while preserving high electrochemical activity. Consequently, the MnO@CNFs electrode exhibits outstanding cycling stability, retaining 81% capacity after 2,500 cycles at a high current density of 1.0 A g^{-1} (Figure 5c). Tang et al.[111] synthesized MnS/MnO@N-doped CNFs (MnS/MnO@N-CNFs) composites via electrospinning, leveraging the carbonization of polyvinylpyrrolidone (PVP) to form the N-doped carbon matrix. The N-doping induces charge redistribution in the carbon matrix, increasing its wettability and electronic conductivity, which contributes to improved cycling stability and rate capability. This cathode material demonstrated improved cycling stability and rate capability for AZIBs.

In parallel with MnO-based systems, MnO_2 has been widely studied due to its high theoretical capacity and relatively large operating voltage.[112–114] However, limited conductivity, poor structural stability, and sluggish Zn^{2+} diffusion hinder its practical application.[115–117] To date, compositing with carbon materials (e.g., graphene, carbon nanotubes, and doped carbons) has proven effective to address these issues by accelerating electron transfer during charge/discharge, thereby enhancing electrode rate capability.[118–121] Among various approaches, integrating MnO_2 with electrospun CNFs has shown particular promise for improving conductivity and structural stability. Yang et al.[122] synthesized flexible carbon films by electrospinning, subsequently converting them into N-doped CNFs through self-assembly and carbonization. K^+-intercalated δ-MnO_2 (KMO) was then in situ grown on the N-CNF surface via a reduction reaction in $KMnO_4$ solution (Figure 5d). The K^+ intercalation expands the interlayer spacing of δ-MnO_2, which reduces the energy barrier for Zn^{2+} diffusion and improves structural stability during cycling. Figure 5e shows the SEM images of the ultrathin KMO. This cathode retained a reversible capacity of 190 mAh g^{-1} after 1,000 cycles at 3 A g^{-1} (Figure 5f). Guo et al.[123] prepared a fast-charging electrode comprising MnO_2 supported on porous CNFs (PCF@MnO_2). This electrode delivered MnO_2-based specific capacities of 326 mAh g^{-1} at 0.1 A g^{-1} and 184 mAh g^{-1} at 1.0 A g^{-1}. Fu et al.[124] employed electrospinning to fabricate PAN fibers, followed by stepwise carbonization to yield CNFs. ε-MnO_2 nanoflowers were subsequently grown hydrothermally on the CNFs to form a 3D ε-MnO_2/CNFs composite. The 3D hierarchical architecture provides a large surface area and abundant active sites, while the intimate contact between ε-MnO_2 and CNFs ensures efficient electron transfer, contributing to the high capacity and cycling stability. The full cell delivered a discharge capacity of 288.6 mAh g^{-1} at 0.2 A g^{-1} and maintained 90.0% capacity retention after 1,000 cycles. In addition to MnO_2, other Mn-based oxides such as Mn_3O_4 have also been explored. Mn_3O_4 exhibits considerable theoretical capacity and a high theoretical voltage versus Zn. Nevertheless, its development for AZIBs has been impeded by rapid capacity fading, primarily caused by dissolution stemming from irreversible side reactions.[113] Long et al.[125] synthesized a core–shell Mn_3O_4@hollow carbon fiber (Mn_3O_4@HCF) composite cathode via coaxial electrospinning, encapsulating Mn_3O_4 nanoparticles within hollow carbon fibers. The hollow carbon fiber effectively confines the Mn_3O_4 nanoparticles, mitigating their dissolution and aggregation, while providing a conductive buffer layer that accommodates volume changes during cycling. The electrode demonstrated stable cycling at 1.5 A g^{-1} for 800 cycles, maintaining a reversible capacity of 131.8 mAh g^{-1}. The Coulombic efficiency (CE) increased to 98.5% within tens of cycles and approached nearly 100% thereafter, indicating high electrochemical reversibility and stability (Figure 5g). Mn_2O_3 nanostructures have also been explored. Wang et al.[126] constructed self-assembled Mn_2O_3 nanofibers composed of Mn_2O_3 nanoparticles via electrospinning followed by calcination. The self-assembled 3D network of Mn_2O_3 nanofibers not only facilitates electron and ion transport but also enhances structural integrity by dissipating mechanical stress during repeated cycling. SEM imaging (Figure 5h) revealed that the prepared Mn_2O_3 nanofibers possess a distinct

© 2025 Wiley-VCH GmbH

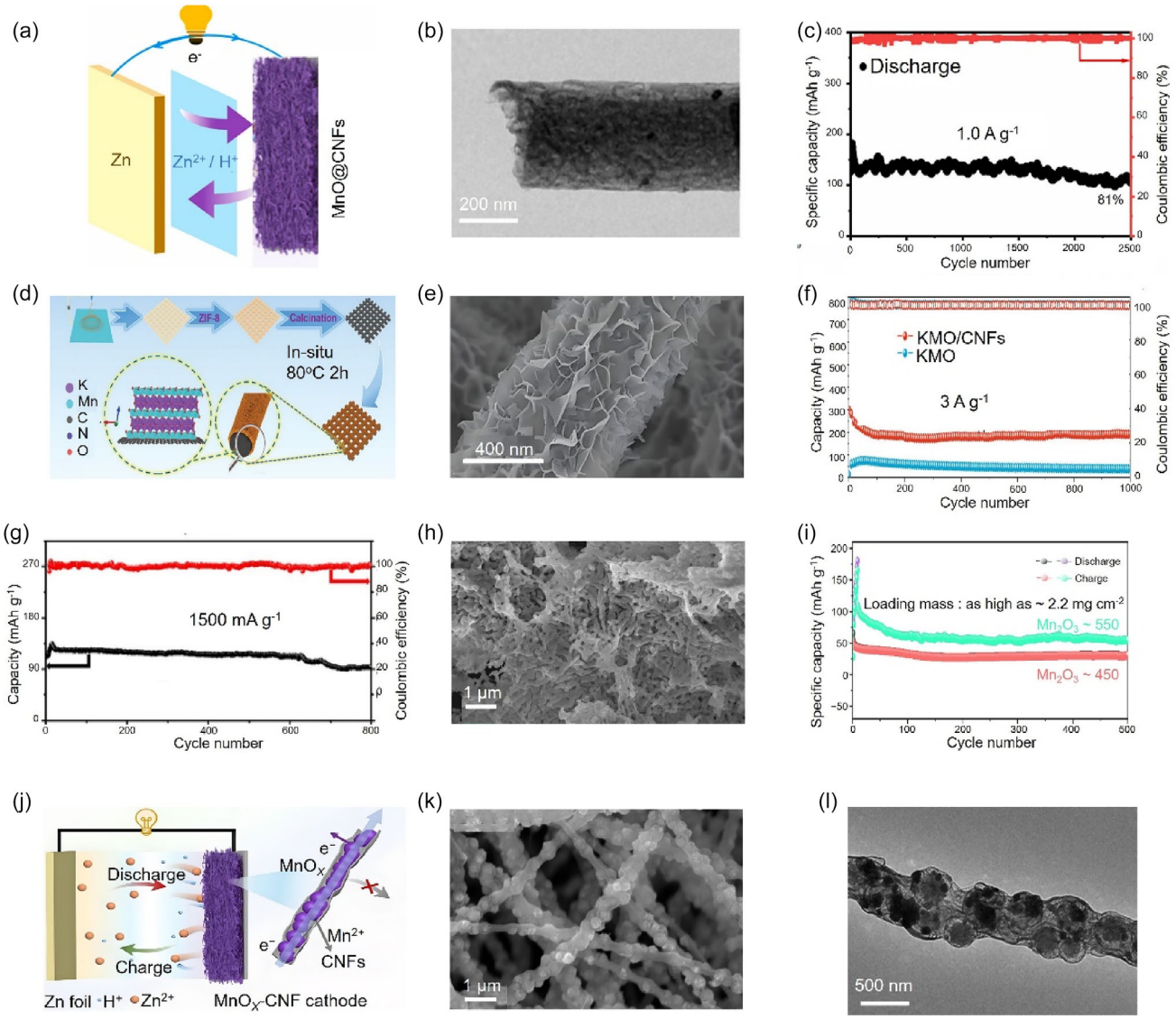

Figure 5. Electrospun nanofibers-enabled Mn-based cathodes for AZIBs. Copyright permissions obtained for figures. a) Schematic illustration of the MnO@CNFs.[110] b) TEM images of the MnO@CNFs.[110] c) Long-term cycling stability over 2,000 cycles tested at high current densities.[110] d) Schematic illustration of the synthesis process for KMO grown on electrospun N-doped CNFs.[122] e) SEM images of the ultrathin KMO/CNFs.[122] f) Long-term cycling performance of KMO/CNFs and KMO at 3.0 A g^{-1}.[122] g) Long-term cycling performance of Mn_3O_4@HCFs electrode at 1,500 mA g^{-1}.[125] h) SEM image of Mn_2O_3 nanofibers.[126] i) Long-term cycling performance of Mn_2O_3-450 and Mn_2O_3-550 electrodes at 1,000 mA g^{-1}.[126] j) Schematic illustration of the MnO_x-CNFs.[107] k) SEM images of the MnO_x-CNFs.[107] l) TEM images of the MnO_x-CNFs.[107]

nanofibrous morphology self-assembled into a 3D network. Employed as a cathode material for AZIBs, the Mn_2O_3 electrode exhibited good Zn^{2+} storage performance, retaining a capacity of 56 mAh g^{-1} after 500 cycles at 1.0 A g^{-1} (Figure 5i). Ding et al.[107] coated CNFs onto bead-like MnO_x particles via electrospinning to enhance electron/ion diffusion kinetics and structural stability (Figure 5j). The core–shell structure with CNFs coating creates a continuous conductive network around each MnO_x particle, ensuring efficient charge transfer while physically suppressing manganese dissolution. Figure 5k shows the SEM images of the MnO_x-CNFs. The core–shell structure of the MnO_x-CNFs revealed by TEM (Figure 5i). This cathode demonstrated remarkable cycling stability, maintaining 71% capacity retention after 5,000 cycles at a high current density of 3 A g^{-1}. Overall, electrospinning has enabled a range of structural and compositional strategies to improve the electrochemical performance of Mn-based oxides in AZIBs. A deeper understanding of the relationship between fiber morphology (diameter, porosity, alignment), composition (doping, vacancy engineering), and electrochemical properties (ionic/electronic conductivity, reaction kinetics, structural stability) is essential for rationally designing high-performance Mn-based cathodes. Continued exploration of tailored electrospinning processes may provide pathways toward more efficient and durable Mn-based cathodes for practical aqueous energy storage applications.

The application of Mn-based electrospun cathodes continues to face several material-specific challenges. Manganese dissolution, which is especially prominent in Mn_3O_4 and MnO_2 systems, remains a major cause of capacity decay during extended

© 2025 Wiley-VCH GmbH

25666223, 0, Downloaded from https://chemistry-europe.onlinelibrary.wiley.com/doi/10.1002/batt.202500655 by University of Ulsan, Wiley Online Library on [11/11/2025]. See the Terms and Conditions (https://onlinelibrary.wiley.com/terms-and-conditions) on Wiley Online Library for rules of use; OA articles are governed by the applicable Creative Commons License

operation. The inherently low electrical conductivity of manganese oxides further limits rate capability, even within carbon-enhanced architectures. At larger scales, difficulties in ensuring uniform active material distribution, tailored porosity, and robust Mn oxide–carbon interfacial bonding become increasingly evident. Moving forward, research should emphasize electrospinning optimization for improved homogeneity and interfacial integrity, exploration of novel Mn-based composites with higher conductivity and stability, and the application of in situ/operando methods to clarify degradation and Zn^{2+} storage mechanisms. Success in these areas is crucial for developing practical Mn-based cathodes.

3.1.3. I_2-Based Cathodes

In recent years, the high redox potential of I_2 (I_2/I^-, 0.62 V vs. SHE) and its large theoretical capacity (211 mAh g^{-1}) have driven increasing interest in combining I_2 with Zn anodes to develop sustainable Zn–I_2 batteries.[127–129] In particular, the conversion reaction of I_2 at the cathode imparts Zn–I_2 batteries with high energy efficiency and distinct advantages over metal-ion batteries. However, Zn–I_2 batteries face challenges including the insulating nature of I_2, low active material utilization, and the polyiodide shuttle effect, leading to rapid capacity decay and severe self-discharge.[130–134] To address these issues, considerable efforts have focused on designing porous carbon matrices to confine I_2 and improve electrochemical kinetics. Electrospinning has served as an effective method to construct such carbon architectures, offering uniform porosity, tunable composition, and mechanical flexibility.[135–137] In one example, Ding et al.[138] employed electrospinning followed by pyrolysis to uniformly disperse iron nitride within flexible porous CNFs. The resulting Zn–I_2 battery delivered a high specific capacity of 214 mAh g^{-1} at a 2 C rate and demonstrated good cycling stability exceeding 1,600 h. MOFs are considered promising precursors for synthesizing heteroatom-doped porous carbons due to their large surface areas, tunable pore sizes, and adaptable structures.[134,139,140] However, thermal decomposition of the organic precursors often causes structural distortion or partial collapse of the MOFs framework, resulting in compromised porosity.[141–144] To mitigate these effects, He et al.[145] integrated an aluminum-based MOF (Al-MOF) with PAN via electrospinning to fabricate Al-MOF/PAN nanofibers, which were subsequently pyrolyzed into N-doped porous CNFs (NPCNFs) (**Figure 6**a). The NPCNFs possessed a hierarchical porous structure and decent flexibility, making them suitable for self-supporting electrodes (Figure 6b). This electrode exhibited enhanced cycling stability in Zn–I_2 battery for over 6,000 cycles with an average CE of 99.4% (Figure 6c). These works highlight the potential of electrospun carbon architectures for stabilizing I_2-based cathodes and mitigating shuttle-induced degradation in aqueous Zn–I_2 batteries.

For Zn–I_2 batteries, electrospun carbon-based cathodes still face persistent issues related to iodine confinement and reaction kinetics. The shuttle effect of polyiodides persists under demanding conditions, such as high current densities or elevated iodine loadings, despite progress in porous host design. Fine control over the pore size distribution and surface chemistry in electrospun CNFs, which is critical for effective iodine trapping and redox facilitation, has proven difficult to achieve. Furthermore, gradual active iodine loss and carbon substrate corrosion during long-term cycling continue to impair durability. Future efforts need to focus on designing host materials with optimized pore architectures and catalytic surfaces, constructing hybrid or multifunctional nanofibers to improve iodine retention and conversion kinetics, and employing advanced in situ techniques to

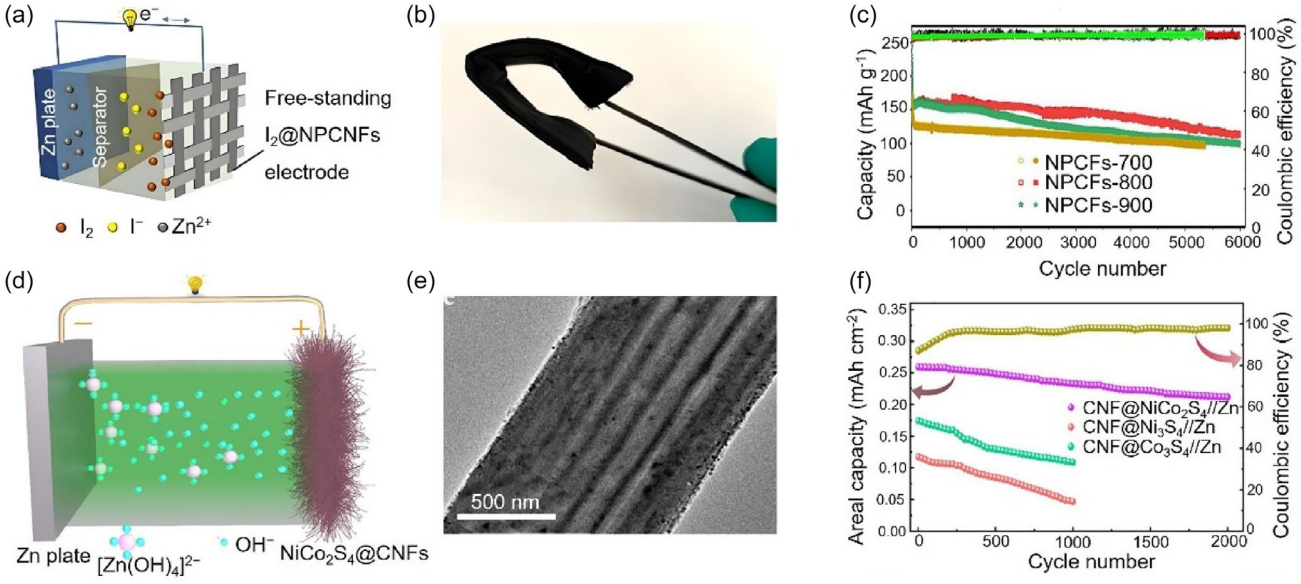

Figure 6. Electrospun nanofibers-enabled I_2-based cathodes for AZIBs. Copyright permissions obtained for figures. a) Schematic illustration for the synthesis process of I_2@NPCNFs to fabricateZn-I_2 battery.[145] b) Photographs of the flexible and freestanding NPCNFs electrode.[145] c) Cycling stability of I_2@NPCNFs-electrodes at 2 C.[145] d) Schematic illustration of the aqueous CNFs@$NiCo_2S_4$//Zn battery.[44] e) TEM images of the CNFs@$NiCo_2S_4$.[44] f) Long-term cycling stability of the CNFs@$NiCo_2S_4$//Zn battery at 10 mA cm^{-2} for 2,000 cycles.[44]

© 2025 Wiley-VCH GmbH

25666223, 0, Downloaded from https://chemistry-europe.onlinelibrary.wiley.com/doi/10.1002/batt.202500655 by University of Ulsan, Wiley Online Library on [11/11/2025]. See the Terms and Conditions (https://onlinelibrary.wiley.com/terms-and-conditions) on Wiley Online Library for rules of use; OA articles are governed by the applicable Creative Commons License

elucidate degradation pathways. Addressing these challenges is key to enabling practical Zn–I_2 batteries.

3.1.4. Ni-Based Cathodes

Ni-based compounds exhibit high theoretical capacity, elevated operating voltage, and substantial energy density, positioning them as promising cathode materials for AZIBs.[146–150] However, their limited conductivity and rapid capacity decay remain critical barriers to practical implementation.[151] Consequently, developing effective strategies to enhance the performance of Ni-based cathodes is imperative. Cui et al.[44] synthesized CNFs-functionalized $NiCo_2S_4$ nanoparticles (CNFs@$NiCo_2S_4$) via electrospinning, yielding a lightweight, flexible, and binder-free cathode material (Figure 6d). Figure 6e shows the TEM images of the CNFs@$NiCo_2S_4$. An aqueous CNFs@$NiCo_2S_4$//Zn battery fabricated using this self-supporting CNFs@$NiCo_2S_4$ film cathode demonstrated high capacity, good rate capability, and long-term cycling stability, retaining 83% capacity after 2,000 cycles at 10 mA cm^{-2} (Figure 6f). Yu et al.[152] first synthesized bimetallic NiCo-MOF spheres via a solvothermal method. These spheres were then integrated with PAN through electrospinning to form bead-on-string structured NiCo-MOF@PAN fibers. Subsequent carbonization under a nitrogen atmosphere produced bimetallic NiCo nanoparticles embedded within hollow carbon spheres anchored on carbon fibers (NiCo/HCS@CFs). Following hydrothermal sulfidation, the NiCo/HCS@CFs were converted into a $NiCo_2S_4$/HCS@CFs film cathode, which exhibited improved rate performance and cycling stability. These studies affirm the utility of electrospun architectures in advancing the performance of Ni-based cathodes under aqueous conditions.

Ni-based electrospun cathodes encounter distinct challenges that impede their practical adoption, including moderate intrinsic electronic conductivity, susceptibility to structural degradation during long-term cycling, and often complex, multistep synthesis routes. Future research must aim to streamline the preparation of these composite fibers, develop more effective material and interface designs to enhance electronic and ionic conduction, and extend cycling stability under high-rate and long-duration operation. A clearer understanding of the energy storage and degradation mechanisms through combined computational and experimental studies will be equally important for performance optimization.

3.1.5. Other Cathodes

This part expands the design landscape of AZIBs cathodes beyond conventional V^-, Mn^-, I_2^-, and Ni-based systems by leveraging electrospun nanofiber architectures. Furthermore, the electrospinning strategy demonstrated here offers valuable insights for next-generation cathode design in other aqueous battery systems. Kim et al.[38] prepared freestanding CNFs via electrospinning and carbonization to support PANI. Leveraging the composite's high conductivity and self-supporting architecture, the PANI/CNFs cathode could be directly employed without binders or conductive additives, enabling battery assembly in arbitrary geometries. Cells incorporating this electrode delivered good rate capability at an ultrahigh 600 C rate. Xu et al.[153] synthesized a composite featuring hybrid carbon-coated $Na_3V_2(PO_4)_3$ (NVP) interconnected with carbon nanotubes. NVP nanoparticles were tightly and randomly encapsulated within CNFs, forming a 3D conductive network that enhanced electronic conductivity and structural stability. Compared to NVP/C, the NVP/C-CNFs electrode demonstrated superior cycling stability. The corresponding full cell retained ≈83.9% capacity after 300 cycles at 1 A g^{-1}, with CE approaching 100%. Wang et al.[48] engineered $Ti_3C_2T_x$@S-V_2O_5@CNF nanofibers (**Figure 7**a) with synergistic effects through concomitant S doping and $Ti_3C_2T_x$ MXene incorporation. This design enhanced aqueous ammonium-ion storage capacity. The assembled full cell ($Ti_3C_2T_x$@S-V_2O_5@CNF//3, 4, 9, 10-perylene-bis(dicarboximide) (PTCDI)) delivered a specific capacity of 181 mAh g^{-1} at 0.5 A g^{-1} and exhibited negligible capacity decay over 10,000 cycles at 5 A g^{-1} (Figure 7b). Li et al.[154] fabricated $Se_{2.9}S_{5.1}$@multichannel CNFs ($Se_{2.9}S_{5.1}$@MCNF) as a cathode for aqueous aluminum-ion batteries via electrospinning followed by calcination and solid-state reaction (Figure 7c). Figure 7d shows the uniformly continuous 1D $Se_{2.9}S_{5.1}$@MCNF with a relatively smooth surface and negligible particle agglomerations, indicating that $Se_{2.9}S_{5.1}$ is homogeneously penetrated in the porous network. The multichannel structure is well retained after introducing $Se_{2.9}S_{5.1}$ as shown in Figure 7e. Comparative analysis with other cathode materials revealed the $Se_{2.9}S_{5.1}$@MCNF electrode's superior cycling stability, attributed to its unique layered structure and favorable interactions with Al^{3+}. The electrode maintained a discharge capacity of 187 mAh g^{-1} after 3,000 cycles, demonstrating exceptional longevity, while CE consistently exceeded 95%, indicating highly reversible electrode reactions.

Together, these studies demonstrate that electrospun nanofiber-enabled cathodes, through tailored composition and architecture, play a pivotal role in enhancing electron/ion transport, confining active species, and maintaining structural integrity, thereby driving the advancement of high-performance AZIBs.

3.2. Anodes

Zn stands out for its low cost, high theoretical capacity, and inherent safety, making it particularly attractive for large-scale energy storage.[155] However, the Zn anode suffers from severe thermodynamic and electrochemical instability in aqueous electrolytes, including corrosion-induced capacity loss and uncontrolled dendrite growth that may lead to short circuits and cell failure.[156,157] These issues critically impair the reversibility and durability of AZIBs, posing substantial barriers to their practical deployment.[158–160]

To address these challenges, researchers have increasingly turned to electrospun nanofiber materials owing to their high structural tunability, mechanical resilience, and ease of surface functionalization. Electrospinning offers versatile platforms for designing protective layers and functional substrates that can regulate Zn deposition, suppress dendrite formation, and improve interfacial stability.

In this context, this section focuses exclusively on electrospun nanofiber-based strategies for Zn anodes, summarizing recent

© 2025 Wiley-VCH GmbH

25666223, 0, Downloaded from https://chemistry-europe.onlinelibrary.wiley.com/doi/10.1002/batt.202500655 by University of Ulsan, Wiley Online Library on [11/11/2025]. See the Terms and Conditions (https://onlinelibrary.wiley.com/terms-and-conditions) on Wiley Online Library for rules of use; OA articles are governed by the applicable Creative Commons License

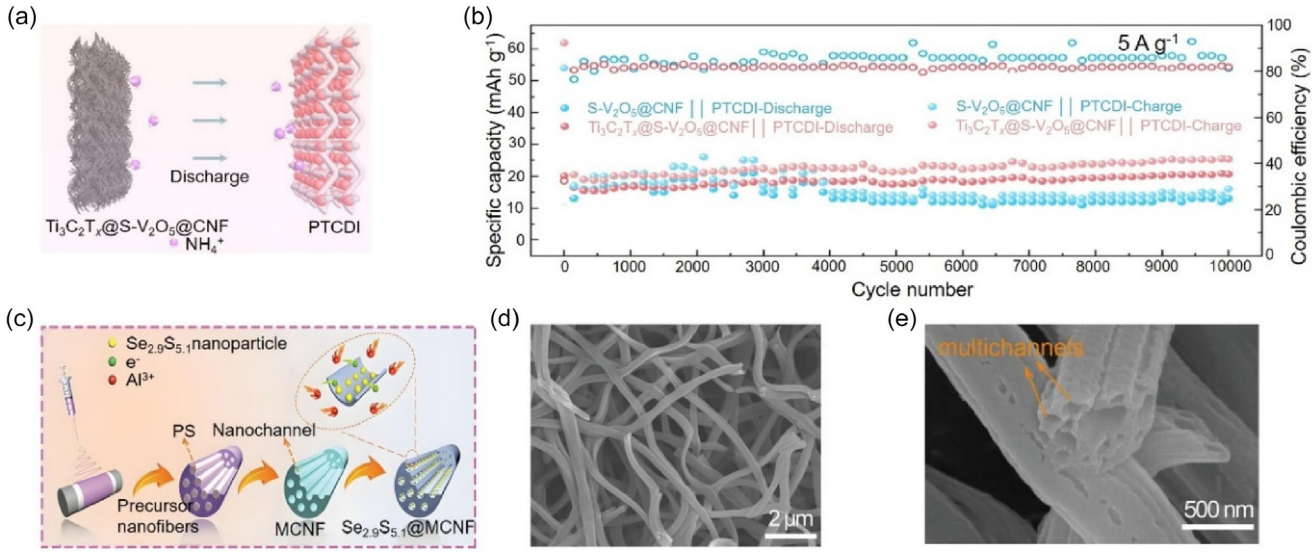

Figure 7. Electrospun nanofibers-enabled other cathodes for AZIBs. Copyright permissions obtained for figures. a) Schematic illustration of the $Ti_3C_2T_x$@S-V_2O_5@CNF//PTCDI and S-V_2O_5@CNF//PTCDI.[48] b) Long-term cycling stability of $Ti_3C_2T_x$@S-V_2O_5@CNF electrodes at 5 Ag^{-1}.[48] c) Schematic illustration of the preparation process of $Se_{2.9}S_{5.1}$@MCNF.[154] d) SEM images of $Se_{2.9}S_{5.1}$@MCNF.[154] e) The magnified SEM image of $Se_{2.9}S_{5.1}$@MCNF.[154]

advances in the design of carbon-based matrices, zincophilic composites, and MXene and polymer-based modified anodes materials tailored to improve the electrochemical performance and stability of Zn anodes in AZIBs.

3.2.1. Electrospun CNFs Scaffolds for Zn Anode

Carbonaceous materials are particularly attractive for electrode substrates due to their low cost, electrochemical/mechanical stability, and versatile chemical modifiability.[161,162] Among them, electrospun CNFs provide have emerged as a particularly effective scaffold for Zn metal anodes. Their large surface area and porous, interconnected architecture reduce local current density, homogenize Zn^{2+} flux, and suppress dendrite growth. These features also stabilize the electrode–electrolyte interface, thereby enhancing cycling reversibility and extending battery lifespan.[163] Building upon the advantages of electrospun CNFs frameworks, several studies have demonstrated their effectiveness in stabilizing Zn deposition and extending anode lifespan. For instance, Sang et al.[164] developed Zn-deposited CNFs (Zn-CNFs) via electrospinning of PAN nanofibers followed by thermal treatment and Zn electrodeposition. As conductive substrates for Zn metal anodes, the Zn-CNFs electrode exhibited 64%–75% lower overpotential during Zn plating/stripping compared to bare Zn in galvanostatic cycling tests. This overpotential reduction persisted at 60.1% after 400 h of operation (**Figure 8**a). Li et al.[165] employed electrospun CNFs as scaffolds to construct Zn@CNFs composite anodes, which effectively suppressed dendrite growth and improved cycling stability. To further enhance Zn deposition behavior, Wang et al.[166] proposed a Zn anode modification strategy featuring a "zincophilic-hydrophobic" PAN-based poly(methyl methacrylate) (PAN/PMMA) membrane protective layer to enable high-rate, dendrite-free Zn anodes. The PAN/PMMA@Zn symmetric cell sustained efficient operation for over 2000 cycles at a current density of 10 mA cm^{-2}, with a low polarization voltage below 65 mV. Collectively, electrospun CNFs scaffolds provide a structurally tunable and electrochemically stable framework that guides uniform Zn deposition, suppresses dendrite growth, and enhances interfacial reversibility, thereby offering a promising design blueprint for high-performance aqueous Zn anodes.

In the realm of Zn metal anodes, the quest for uniform Zn deposition remains fraught with challenges, particularly under high current densities and prolonged cycling. Interfacial side reactions and the scalability of electrospun scaffolds with well-defined pore and surface characteristics also present hurdles. Future development should center on refining the surface chemistry and hierarchical porosity of CNFs to strengthen zincophilicity and ion transport, alongside innovating more efficient and scalable fabrication methods to meet the demands of practical Zn-based energy storage devices.

3.2.2. Zincophilic Modifications of Electrospun CNFs for Zn Anodes

To further enhance the Zn affinity and interfacial stability of carbon-based anodes, various zincophilic materials have been integrated into electrospun CNFs scaffolds. Ye et al.[167] fabricated Bi–Bi_2O_3@CNF composites with hierarchical hollow structures and surface grooves through integrated electrospinning, thermal treatment, and in situ growth (Figure 8b). The introduction of Bi–Bi_2O_3 significantly enhanced electrochemical performance, reducing polarization overpotential by 17.6%, increasing hydrogen evolution overpotential by 11.5%, and maintaining 98.8% CE over prolonged cycling compared to pristine Zn anodes. Symmetric Zn@Bi–Bi_2O_3@CNF cells exhibited stable voltage profiles exceeding 200 h at 10 and 20 mA cm^{-2} (Figure 8c), while full

© 2025 Wiley-VCH GmbH

25666223, 0, Downloaded from https://chemistry-europe.onlinelibrary.wiley.com/doi/10.1002/batt.202500655 by University of Ulsan, Wiley Online Library on [11/11/2025]. See the Terms and Conditions (https://onlinelibrary.wiley.com/terms-and-conditions) on Wiley Online Library for rules of use; OA articles are governed by the applicable Creative Commons License

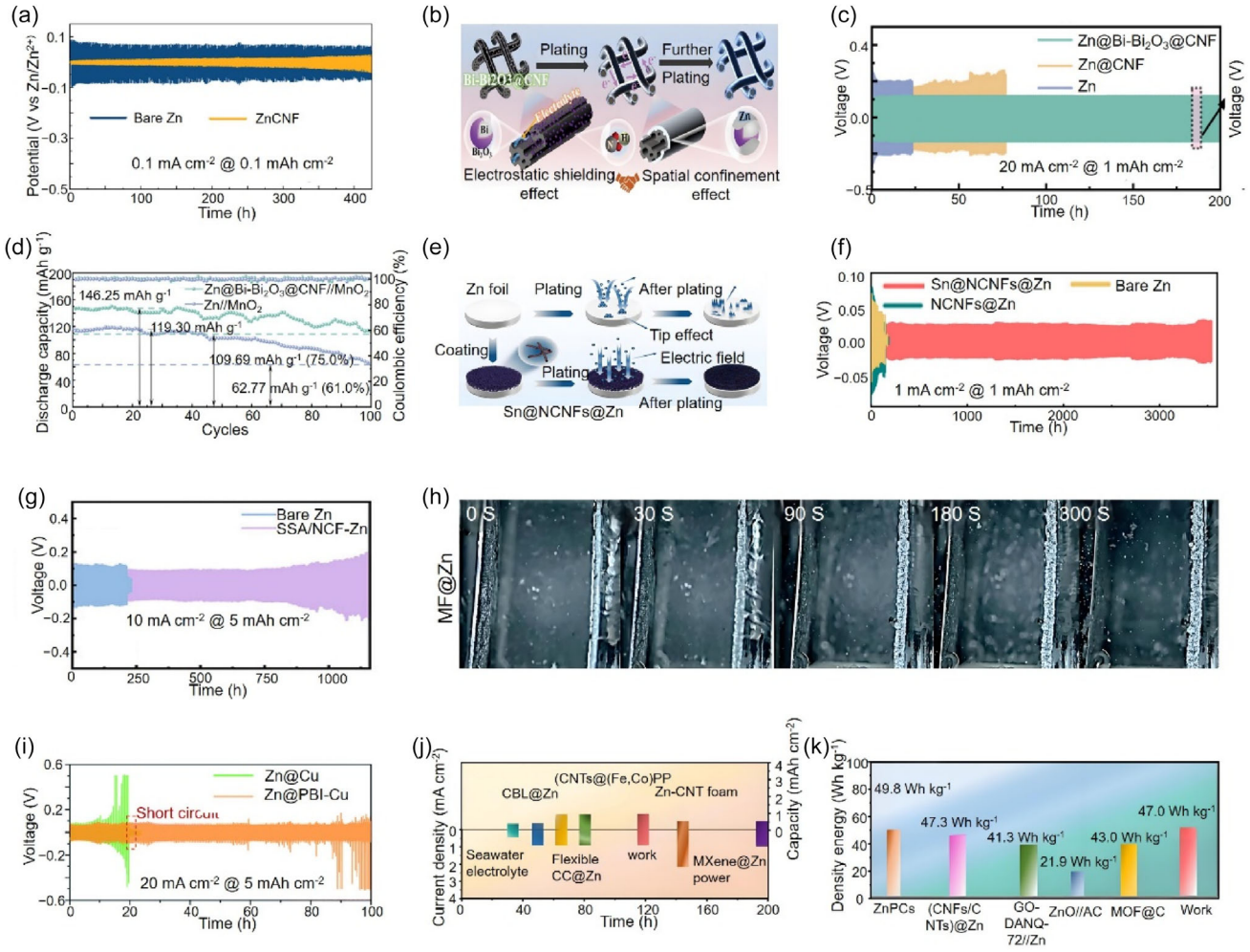

Figure 8. Electrospun nanofiber-based strategies for stable Zn anodes. Copyright permissions obtained for figures. a) Long-term cycling stability of the ZnCNF.[164] b) Schematic illustration of the mechanisms for Bi–Bi_2O_3@CNF.[167] c) Long-term cycling stability of Zn@Bi–Bi_2O_3@CNF, Zn@CNF, and Bare Zn in symmetric cells: charge–discharge voltage profiles at current densities of 20 mA cm^{-2}.[167] d) Galvanostatic charge–discharge cycling curves at 200 mA g^{-1}.[167] e) Schematic illustration of the typical Zn deposition process.[171] f) Long-term cycling stability of Zn||Zn, NCNFs@Zn||NCNFs@Zn, and Sn@NCNFs@Zn||Sn@NCNFs@Zn symmetric cells at 1.0 mA cm^{-1} and 1.0 mAh cm^{-2}.[171] g) Long-term cycling stability of symmetric cells at current densities/capacities of 10 mA cm^{-2}/5 mAh cm^{-2}.[173] h) In situ optical microscopy visualization of Zn plating on raw Zn and MF@Zn electrode at 5 mA cm^{-2}.[178] i) Long-term cycling stability of symmetrical Zn@PBI-Cu and Zn@Cu cells at a current density of 20 mA cm^{-2} with an areal capacity of 5 mAh cm^{-2}.[57] j) Lifespans of PF@Zn//PF@Zn symmetrical cell under different conditions in comparison with previous literatures.[180] k) Comparison of mass energy density of different capacitors.[180]

Zn@Bi–Bi_2O_3@CNF//MnO_2 cells retained 75.0% capacity after 100 cycles at 200 mA g^{-1} (Figure 8d).

Recent advances have highlighted N[168,169] and Sn[170] as zincophilic mediators for dendrite suppression, with Sn further inhibiting hydrogen evolution reaction (HER) kinetics to extend battery lifespan. Wang et al.[171] engineered Sn-embedded N-doped CNFs (Sn@NCNFs) via electrospinning as artificial anode protective layers. The N-doped carbon framework homogenizes local current density and Zn^{2+} flux, while Sn nanoparticles enable low nucleation overpotential (29.1 mV at 1.0 mA cm^{-2} vs. 48.6 mV for bare Zn) and HER suppression, collectively guiding dendrite-free deposition (Figure 8e). The Sn@NCNFs@Zn symmetric cell sustained minimal voltage hysteresis (≈40 mV) and stable cycling for >3,000 h at 1.0/1.0 mAh cm^{-2} (Figure 8f). Other zincophilic materials, such as SiO_2, have also shown promise by redirecting ion flux and reinforcing mechanical integrity.[172] Zhu et al.[173] developed electrospun 3D beaded SiO_2@SiO_2/C N-doped fibers (SSA/NCF) as multifunctional coatings, achieving 1,160 h stability at 10/5 mAh cm^{-2}, which was 5.5× longer than bare Zn anode (Figure 8g). Complementary strategies include Cu@CNFs coatings for current density homogenization[174] and Rao et al.'s gelatin-derived amorphous VO_x embedded within N-doped CNFs framework (VO_x@GC) nanofibers[175] for prolonged Zn anode lifespan exceeding 4,000 h. These advancements demonstrate that integrating zincophilic components into electrospun CNFs scaffolds offers a promising route to stabilize Zn anodes by promoting uniform Zn nucleation, suppressing side reactions, and extending cycling longevity.

While zincophilic modifications offer a promising route to stabilize Zn anodes, maintaining long-term performance under high current densities and deep cycling conditions remains difficult. The scalable and economical production of composite scaffolds

© 2025 Wiley-VCH GmbH

25666223, 0, Downloaded from https://chemistry-europe.onlinelibrary.wiley.com/doi/10.1002/batt.202500655 by University of Ulsan, Wiley Online Library on [11/11/2025]. See the Terms and Conditions (https://onlinelibrary.wiley.com/terms-and-conditions) on Wiley Online Library for rules of use; OA articles are governed by the applicable Creative Commons License

is similarly challenging. Another critical issue is the precise control over the distribution and electrochemical stability of zincophilic nanoparticles within the nanofiber matrix. Research going forward should prioritize the development of more robust and conductive zincophilic materials, the design of hierarchical and multifunctional fiber architectures to coordinately regulate ion transport and deposition, and the fundamental investigation of interfacial stabilization mechanisms via in situ characterization and modeling. These steps are essential to advance modified electrospun CNFs into practical Zn anodes.

3.2.3. MXene and Polymer-Based Modified Anodes Materials

MXene, a novel 2D material characterized by its rich surface functional groups and distinct physicochemical properties, is being explored for battery surface protection.[176,177] Recently, Sha et al.[178] demonstrated a method to directly construct 3D MXene fibrous whiskers on Zn foil surfaces (MF@Zn) via electrospinning to suppress Zn dendrite growth. In situ optical microscopy observations provided direct visual evidence of the effectiveness of the MF@Zn electrode in inhibiting dendrite formation (Figure 8h). Under high current density (5 mA cm^{-2}) and high areal capacity (5 mAh cm^{-2}) conditions, the MF@Zn symmetric battery can stably cycle for over 200 h without short-circuiting, whereas the raw Zn electrode can only cycle for ≈50 h under the same conditions. Jian et al.[57] developed a Zn anode architecture by PBI nanofiber scaffold directly onto a Cu substrate. The PBI nanofibers adhere to the Cu surface, providing uniform nucleation sites for Zn deposition. Furthermore, the polar functional groups on the PBI polymer attract Zn^{2+} ions from the electrolyte, promoting their uniform transport within the porous PBI framework through an electrokinetic effect.[179] Symmetrical cells employing this electrode exhibited stable charge/discharge profiles at 20 and 5 mAh cm^{-2}, cycling stably for over 80 h (Figure 8i). Sha et al.[180] also reported a strategy utilizing electrospinning to weave Zn powder into PAN/polyvinylidene fluoride (PAN/PVDF) fibrous filaments, fabricating a 3D porous Zn anode (PF@Zn). Parameters such as voltage, flow rate, temperature, and humidity during spinning were carefully controlled to achieve a uniform and dense fiber membrane. The resulting 3D fibrous framework is both stable and flexible, preventing direct electrolyte contact with the current collector, mitigating stress from dendrite growth, and uniformly distributing Zn powder within the fiber network. This effectively homogenizes the Zn^{2+} flux, enabling stable Zn cycling. Comparative analysis of the cycling lifespan of PF@Zn symmetrical cells against other synthetic Zn anodes highlighted the superior stability of the PF@Zn anode. In contrast, the other anodes exhibited higher voltage fluctuations and shorter cycle lives during operation, with some failing prematurely due to short circuits or rapid performance degradation (Figure 8j). Furthermore, comparisons of mass energy density across different capacitors underscored the exceptional performance of capacitors based on the PF@Zn anode (Figure 8k).

Electrospun nanofiber-based architectures offer versatile strategies to stabilize Zn anodes. Through engineering carbon frameworks, incorporating zincophilic components, and integrating functional materials such as MXene and polymers, these designs promote uniform Zn deposition, suppress dendrite formation, and enhance long-term cycling stability, contributing to the advancement of reliable AZIBs. Protective layers based on MXene or polymer nanofibers, despite their potential, introduce their own set of challenges pertaining to material stability, scalable integration, and cost-effectiveness. Future work must concentrate on enhancing the durability and ionic conductivity of these protective barriers, optimizing electrospinning parameters for reproducible large-scale manufacture, and deepening the fundamental insight into interfacial ion regulation mechanisms. These advances are necessary to realize durable, high-performance Zn anodes for practical applications.

3.3. Separators

In AZIBs, the separator plays a crucial role by physically isolating the electrodes while regulating ionic transport and retaining the electrolyte. Its performance significantly impacts overall cell stability, CE, and energy density.[181] This part also centers on separators for AZIBs, consistent with the focus on anodes, given their relevance to large-scale energy storage and the critical role of separator design in mitigating dendrite formation and side reactions in aqueous systems. Glass fiber are widely used in AZIBs due to their favorable electrolyte affinity and decent ionic conductivity. However, their porous structure often traps Zn^{2+} during stripping, leading to the formation of inactive "dead Zn" and contributing to capacity fade.[182] Additionally, their high electrolyte uptake increases the battery mass, compromising energy density.[25] Although filter paper and nonwoven separators possessgood mechanical properties and high porosity, their broader application is hindered by poor ion transport regulation capabilities. Compared to conventional separators, electrospun polymer nanofiber separators have attracted significant attention due to their thermal stability, mechanical robustness, electronic insulation, high mechanical elasticity, and controllable structure.[183–185]

3.3.1. PAN and its Modified Separators

PAN, known for its electrochemical and mechanical stability, is one of the most extensively used materials for electrospun nanofiber separators. Recent studies have explored a variety of PAN-based modifications to address dendrite growth, side reactions, and cycling stability. For instance, Fang et al.[29] utilized electrospinning to prepare a PAN nanofiber separator featuring a long-range ordered 3D structure. The uniformly distributed N atoms on the PAN separator surface homogenize ion flux and guide cation transport via N—Zn bonding, thereby promoting a uniform electric field distribution across the anode (**Figure 9**a). Zn symmetric cells incorporating this separator demonstrated a lower nucleation overpotential during extended cycling tests (Figure 9b). Full cells exhibited an 89.2% capacity retention after 1,500 cycles at 10 A g^{-1}. Building upon this framework, Yao et al.[58] developed a separator based on PAN/graphene oxide (PG) composite nanofibers to regulate Zn^{2+} migration and distribution within the

© 2025 Wiley-VCH GmbH

25666223, 0, Downloaded from https://chemistry-europe.onlinelibrary.wiley.com/doi/10.1002/batt.202500655 by University of Ulsan, Wiley Online Library on [11/11/2025]. See the Terms and Conditions (https://onlinelibrary.wiley.com/terms-and-conditions) on Wiley Online Library for rules of use; OA articles are governed by the applicable Creative Commons License

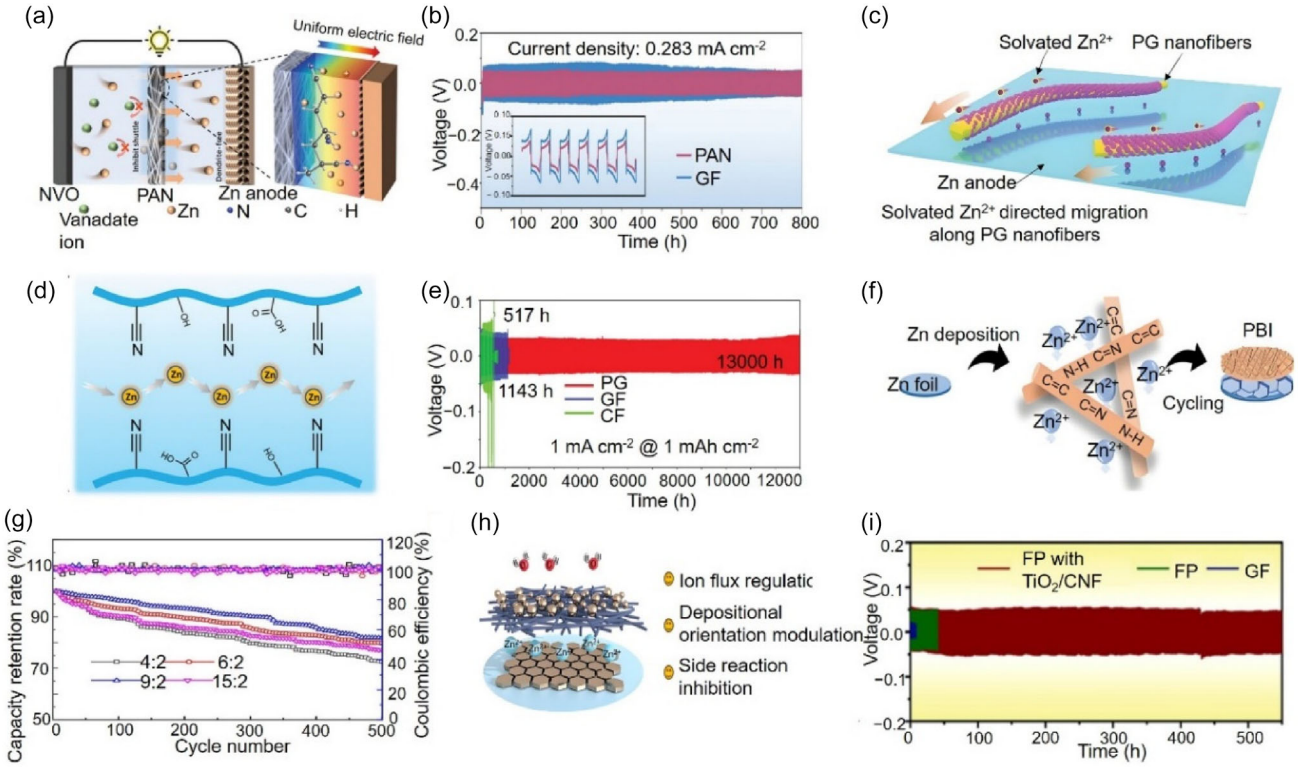

Figure 9. Electrospun nanofiber-based separators for AZIBs. Copyright permissions obtained for figures. a) The working mechanism of PAN separator.[29] b) Cycling performance of Zn/PAN/Zn symmetric cell.[29] c,d) Schematic illustration of solvated Zn^{2+} migrating along the directed migration paths of PG nanofibers targeting stabilized Zn anode.[58] e) Long-term cycling stability of Zn||Zn symmetric cells with PG separator at 1 mA cm^{-2} for 1 mAh cm^{-2}.[58] f) Schematic illustration of Zn plating/stripping behaviors of Zn anodes with PBI separator.[190] g) Capacity retention rate (left) and coulomb efficiency (right), AZIBs assemble by PTFE/PVA derived nanofibers separator.[191] h) Mechanism of the TiO_2/CNF separator promoting uniform Zn deposition and suppressing dendrites.[47] i) Long-term cycling stability at current density of 2 mA cm^{-2} and capacity of 1 mA cm^{-2}.[47]

separator, thereby suppressing uncontrolled Zn growth (Figure 9c, d). Zn||Zn symmetric cells using the PG separator achieved an ultra-stable cycling lifespan exceeding 13,000 h (Figure 9e). This highlights the benefit of incorporating conductive and functional nanofillers to tune separator microenvironments.

Beyond structural modifications, surface chemistry has also been tailored. Wu et al.[186] fabricated PAN/SiO_2 composite separators with varying SiO_2 contents using electrospinning followed by a rolling process. The hydrophobic nature and dense structure of these separators effectively suppressed corrosion and the HER, reducing side-product formation. Building on the strategy of interfacial regulation through chemical functionalization, Cheng et al.[187] introduced a zwitterionic surfactant into the PAN matrix. The resulting PAN-zwitterionic surfactant separator improved interfacial compatibility and ion mobility, contributing to enhanced overall electrochemical performance. Efforts have also shifted toward constructing composite structures that integrate multiple functional components within the PAN nanofiber network. Li et al.[188] designed a synergistic PAN-Zn trifluoro methane sulfonate (ZnTFSI) nanofiber/glass fiber (PZ-GF) separator to regulate Zn deposition behavior and improve cell performance. Furthermore, to regulate electron distribution at the electrode–separator interface, Wang et al.[189] incorporated graphite nanoparticles into PAN to develop a modified PAN nanofiber separator (GPAN) via electrospinning. The graphite nanoparticles function as an electron buffer layer, accelerating interfacial charge transfer, dispersing excess charge on the electrode surface, reducing polarization induced by charge accumulation, and suppressing tip effects through electron dissipation.

Overall, PAN-based nanofiber separators, especially when combined with functional additives, enable controlled Zn^{2+} transport and interface stabilization, offering a promising route for enhancing the performance in AZIBs.

3.3.2. Other Electrospun Polymer Separators

While PAN is widely used for electrospun separators, alternative polymers offer distinct advantages tailored to specific challenges in AZIBs. For instance, polybenzimidazole (PBI) possesses thermal stability and mechanical strength, which is crucial for enhancing battery safety. In contrast, polytetrafluoroethylene/poly (vinyl alcohol) (PTFE/PVA) systems are chemically inert and hydrophobic. This property suppresses water-induced side reactions, such as Zn corrosion and hydrogen evolution, thereby improving cycling stability. These materials provide complementary properties to PAN, addressing its limitations in harsh electrochemical environments. Hussain et al.[190] synthesized PBI polymer via polycondensation and subsequently fabricated a PBI nanofiber separator using electrospinning (Figure 9f). In symmetric cell testing, the PBI separator significantly enhanced the reversibility and

© 2025 Wiley-VCH GmbH

25666223, 0, Downloaded from https://chemistry-europe.onlinelibrary.wiley.com/doi/10.1002/batt.202500655 by University of Ulsan, Wiley Online Library on [11/11/2025]. See the Terms and Conditions (https://onlinelibrary.wiley.com/terms-and-conditions) on Wiley Online Library for rules of use; OA articles are governed by the applicable Creative Commons License

cycling stability of Zn deposition/stripping, achieving a cycle life exceeding 400 h at a current density of 5 mA cm^{-2}. Wang et al.[191] prepared a PTFE/PVA-derived nanofiber separator via emulsion electrospinning followed by sintering. The PTFE/PVA nanofiber separator, optimized at a PTFE:PVA mass ratio of 9:2, demonstrated decent overall electrochemical performance in AZIBs. This included low internal resistance (≈2 Ω), good power retention (42.74 Wh kg^{-1} at 600 W kg^{-1}), high capacity retention (≥82%), and high CE (≥99%) after 500 cycles (Figure 9g). Collectively, these polymer-based nanofiber separators demonstrate how tailored composition and architecture can effectively address interfacial challenges and improve long-term performance in AZIBs systems.

3.3.3. Inorganic-Modified Separators

To further enhance ionic conductivity and interfacial control, inorganic components have been incorporated into nanofiber matrices. The incorporation of inorganic nanoparticles can improve the separator's affinity for the aqueous electrolyte, ensuring better pore-filling and thus a lower interfacial resistance. Liu et al.[47] employed electrospinning to fabricate a titanium dioxide fiber membrane (TiO_2/CNF) with a 3D network structure. This TiO_2/CNF layer was combined with filter paper to form a composite separator. The TiO_2/CNF interlayer, featuring abundant pores and a 3D network, facilitates uniform Zn^{2+} transport. The inherent zincophilicity of TiO_2 guides Zn deposition along the (002) crystal plane, promoting uniform Zn deposition. Furthermore, the TiO_2/CNF interlayer acts as a protective layer, suppressing side reactions and Zn dendrite growth (Figure 9h). Zn||Zn symmetric cells employing this TiO_2/CNF-modified separator exhibited stable cycling for 650 h at a current density of 2 mA cm^{-2} (Figure 9i).

The integration of inorganic nanoparticles into nanofiber matrices for separators or modifiers, although beneficial, is constrained by difficulties in achieving uniform nanoparticle dispersion and strong interfacial adhesion within the polymer fiber matrix. Furthermore, balancing high ionic conductivity with adequate mechanical strength in such composite fibers is nontrivial. Subsequent research should pursue more effective hybrid material designs, optimize the composition and spatial distribution of nanoparticles, and acquire a deeper understanding of the ion transport and deposition behavior at modified interfaces.

4. Summary and Perspectives

Electrospinning has emerged as a versatile and powerful strategy for engineering nanostructured materials in AZIBs. This review has systematically examined the progress in electrospun nanofibers applied to key battery components. The integration of electrospun nanofibers into cathodes enable improved electronic conductivity, structural stability, and ion accessibility across a broad range of

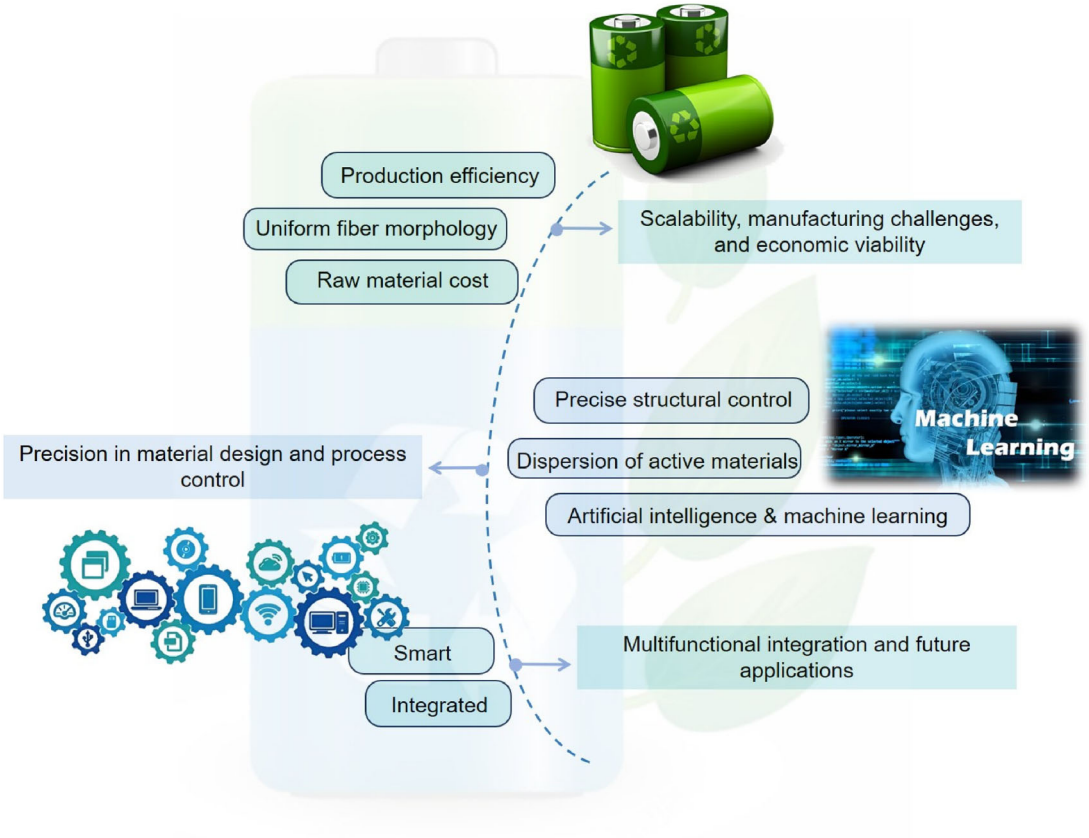

Figure 10. The future of electrospinning in AZIBs technology: key development directions.

© 2025 Wiley-VCH GmbH

25666223, 0, Downloaded from https://chemistry-europe.onlinelibrary.wiley.com/doi/10.1002/batt.202500655 by University of Ulsan, Wiley Online Library on [11/11/2025]. See the Terms and Conditions (https://onlinelibrary.wiley.com/terms-and-conditions) on Wiley Online Library for rules of use; OA articles are governed by the applicable Creative Commons License

active materials including V-, Mn-, I_2-, and Ni-based systems. On the anode side, electrospun carbon frameworks and zincophilic modifications have demonstrated effectiveness in guiding uniform Zn deposition and suppressing dendrite formation for AZIBs. Similarly, electrospun separators, particularly those based on PAN and its composites, offer tunable porosity, enhanced electrolyte wettability, and regulated ion transport. Together, these advances underscore the unique advantages of electrospun architectures in optimizing interface chemistry and transport dynamics within AZIBs. Despite these achievements, its further development and practical application still face considerable challenges (**Figure 10**).

4.1. Scalability, Manufacturing Challenges, and Economic Viability

This subsection addresses the primary obstacles hindering the large-scale application of electrospinning in AZIBs. Conventional electrospinning processes suffer from low production efficiency, which falls short of the volume requirements for commercial-scale electrode and separator manufacturing. Although advanced strategies such as multineedle and needleless electrospinning have improved output, issues related to fiber uniformity, reproducibility, and consistency over large areas remain unresolved. Furthermore, the relatively high cost of high-performance polymers or precursors undermines economic viability, particularly in cost-sensitive markets. Future developments should emphasize scalable, low-cost, and ecofriendly manufacturing approaches, such as melt electrospinning, aqueous electrospinning, and the adoption of biomass-derived materials, to strengthen competitiveness and minimize environmental footprint.

4.2. Precision in Material Design and Process Control

A critical challenge lies in the precise control of fiber characteristics, including diameter, orientation, porosity, and pore size distribution, especially for complex architectures such as core–shell, hollow, or Janus structures. Attaining high active material loading with homogeneous dispersion and well-defined interfacial properties remains difficult. Advancements rely on innovative processing techniques complemented by in situ characterization. Furthermore, incorporating artificial intelligence and machine learning for real-time monitoring and adaptive control could significantly improve process precision, product consistency, and facilitate standardized evaluation systems essential for industrial translation.

4.3. Multifunctional Integration and Future Applications

Looking beyond conventional roles, electrospun nanofibers hold promise for multifunctional energy storage systems. Emerging applications include self-healing electrodes/separators that autonomously repair cycling-induced degradation, thermal-responsive separators for safe operation under extreme conditions, and integrated devices combining energy harvesting and storage. These innovative designs not only enhance battery performance and safety but also open new avenues for smart and integrated energy solutions.

Acknowledgements

This work was supported by the Beijing Natural Science Foundation (2232037, F252071, 2242041, 2232054) and Fundamental Research Funds for the Central Universities (FRF-GF-25−014).

Conflict of Interest

The authors declare no conflict of interest.

Keywords: aqueous zinc ion batteries · electrode materials · electrospinning · nanofibers

[1] B. Dunn, H. Kamath, J. M. Tarascon, *Science* **2011**, *334*, 928.
[2] C. Bauer, S. Burkhardt, N. P. Dasgupta, L. A.-W. Ellingsen, L. L. Gaines, H. Hao, R. Hischier, L. Hu, Y. Huang, J. Janek, C. Liang, H. Li, J. Li, Y. Li, Y.-C. Lu, W. Luo, L. F. Nazar, E. A. Olivetti, J. F. Peters, J. L. M. Rupp, M. Weil, J. F. Whitacre, S. Xu, *Nat. Sustain.* **2022**, *5*, 176.
[3] M. Li, J. Lu, Z. Chen, K. Amine, *Adv. Mater.* **2018**, *30*, 1800561.
[4] Y. Mao, Y. Zhang, M. Su, Y. Ning, J. Shao, K. Zhu, S. Lou, *Energy Environ. Sci.* **2025**, *18*, 8631.
[5] L. Schlott, M. Gutsch, J. Leker, *Nat. Rev. Clean Technol.* **2025**, *1*, 656.
[6] L. Zeng, *Nat. Rev. Clean Technol.* **2025**, *1*, 114.
[7] J. Deng, C. Bae, J. Marcicki, A. Masias, T. Miller, *Nat. Energy* **2018**, *3*, 261.
[8] Y. Liang, Y. Yao, *Nat. Rev. Mater.* **2023**, *8*, 109.
[9] K. Turcheniuk, D. Bondarev, V. Singhal, G. Yushin, *Nature* **2018**, *559*, 467.
[10] B. Y. Tang, L. T. Shan, S. Q. Liang, J. Zhou, *Energy Environ. Sci.* **2019**, *12*, 3288.
[11] L. W. Jiang, S. Han, Y. C. Hu, Y. Yang, Y. X. Lu, Y. C. Lu, J. M. Zhao, L. Q. Chen, Y. S. Hu, *Nat. Energy* **2024**, *9*, 839.
[12] Z. Wu, J. Liu, *Batteries Supercaps* **2024**, *7*, e202400483.
[13] R. F. Service, *Science* **2021**, *372*, 890.
[14] Y. L. Liang, Y. Jing, S. Gheytani, K. Y. Lee, P. Liu, A. Facchetti, Y. Yao, *Nat. Mater.* **2017**, *16*, 841.
[15] G. J. Liang, F. N. Mo, X. L. Ji, C. Y. Zhi, *Nat. Rev. Mater.* **2021**, *6*, 109.
[16] X. K. Zhang, P. C. Xing, T. L. Madanu, J. Li, J. Shu, B. L. Su, *Natl. Sci. Rev.* **2023**, *10*, nwad235.
[17] Y. N. Chen, S. Zhou, J. W. Li, X. Zhang, C. C. Zhou, X. D. Shi, C. X. Zhang, G. Z. Fang, S. Q. Liang, Z. Su, A. Q. Pan, *Angew. Chem. Int. Ed.* **2025**, *64*, e202423252.
[18] T. Zhou, L. Zhu, L. Xie, Q. Han, X. Yang, L. Chen, G. Wang, X. Cao, *J. Colloid Interface Sci.* **2022**, *605*, 828.
[19] X. Wang, R. Jommongkol, J. Deng, K. Liu, J. Qian, Y. Zhu, O. Fontaine, *Batteries Supercaps* **2025**, *8*, e202400722.
[20] N. Kiatwisarnkij, Z. Song, C. Tangpongkitjaroen, S. Wannapaiboon, X. Zhang, P. Wangyao, J. Qin, *Batteries Supercaps* **2025**, *8*, e202400727.
[21] P. Yu, J. Wang, X. Gan, Z. Guo, L. Huang, Z. Song, *Batteries Supercaps* **2023**, *6*, e202300010.
[22] J. F. Parker, C. N. Chervin, I. R. Pala, M. Machler, M. F. Burz, J. W. Long, D. R. Rolison, *Science* **2017**, *356*, 415.
[23] S. Sariyer, S. Yeşilot, N. Kılıç, A. Ghosh, O. Sel, R. Demir-Cakan, *Batteries Supercaps* **2023**, *6*, e202200529.
[24] Q. Ni, B. Kim, C. A. Wu, K. Kang, *Adv. Mater.* **2022**, *34*, e2108206.
[25] L. Li, S. Jia, Z. Cheng, C. Zhang, *ChemSusChem* **2023**, *16*, e202202330.
[26] J. Heo, D. Dong, Z. Wang, F. Chen, C. Wang, *Joule* **2025**, *9*, 101844.
[27] Y. Wang, W. Chen, F. Wang, X. Li, Z. Zhang, W. Li, F. Wang, *Adv. Mater.* **2025**, *37*, 2500596.
[28] R. Wang, Y. Liu, Q. Luo, P. Xiong, X. Xie, K. Zhou, W. Zhang, L. Zhang, H. J. Fan, C. Zhang, *Adv. Mater.* **2025**, *37*, 2419502.
[29] Y. Fang, X. S. Xie, B. Y. Zhang, Y. Z. Chai, B. A. Lu, M. K. Liu, J. Zhou, S. Q. Liang, *Adv. Funct. Mater.* **2022**, *32*, 2109671.

© 2025 Wiley-VCH GmbH

25666223, 0, Downloaded from https://chemistry-europe.onlinelibrary.wiley.com/doi/10.1002/batt.202500655 by University of Ulsan, Wiley Online Library on [11/11/2025]. See the Terms and Conditions (https://onlinelibrary.wiley.com/terms-and-conditions) on Wiley Online Library for rules of use; OA articles are governed by the applicable Creative Commons License

[30] L. Zijian, L. Mingyang, H. Wanyu, F. Bin, *Energy Mater.* **2025**, *5*, 500069.
[31] H. Jia, K. Y. Liu, Y. Lam, B. Tawiah, J. H. Xin, W. Q. Nie, S. X. Jiang, *Adv. Fiber Mater.* **2023**, *5*, 36.
[32] J. Zhao, Z. Yuan, J. Wu, L. Tong, X. Li, M. Wang, M. Li, X. Li, Z. Li, X. Chen, Y. Chen, *ACS Nano* **2025**, *19*, 8266.
[33] D. Kong, W. Guo, Y. Zhao, Y. Zhao, *Adv. Energy Mater.* **2025**, *15*, 2403983.
[34] F. Zhang, Y. Si, J. Yu, B. Ding, *Chem. Eng. J.* **2023**, *456*, 140989.
[35] J. Xue, T. Wu, Y. Dai, Y. Xia, *Chem. Rev.* **2019**, *119*, 5298.
[36] C. Wang, W. Wang, H. Qi, Y. Dai, S. Jiang, B. Ding, X. Wang, C. Li, J. Zeng, T. Wu, H. Li, Y. Wang, Y. Zhao, W. Wang, Z. Li, X. Mo, H. Hou, L. Dong, H. Ma, Y. Liu, C. Su, J. Bai, W. Wu, G. Guo, G. Nie, N. Wang, H. Zhu, J. Bai, J. Fang, D. Liang, et al., *Prog. Mater. Sci.* **2025**, *154*, 101494.
[37] P. Hiralal, S. Imaizumi, H. E. Unalan, H. Matsumoto, M. Minagawa, M. Rouvala, A. Tanioka, G. A. J. Amaratunga, *ACS Nano* **2010**, *4*, 2730.
[38] C. Kim, B. Y. Ahn, T. S. Wei, Y. Jo, S. Jeong, Y. Choi, I. D. Kim, J. A. Lewis, *ACS Nano* **2018**, *12*, 11838.
[39] Q. P. Jian, Y. H. Wan, J. Sun, M. C. Wu, T. S. Zhao, *J. Mater. Chem. A* **2020**, *8*, 20175.
[40] Z. Y. Chen, J. G. Hu, S. J. Liu, H. S. Hou, G. Q. Zou, W. T. Deng, X. B. Ji, *Chem. Eng. J.* **2021**, *404*, 126536.
[41] Y. Hu, Y. Ren, R. Shi, J. Yu, Z. Sun, S. Guo, J. Guo, F. Yan, *ACS Appl. Mater. Interfaces* **2021**, *13*, 16289.
[42] T. Ma, Y. Xiao, X. Lv, H. Yue, Y. Huang, X. Li, N. He, C. Zhan, Y. Bai, D. Nan, *Batteries Supercaps* **2025**, *8*, e202400726.
[43] Z. Ma, J. Yuan, *ChemElectroChem* **2025**, *12*, e202500125.
[44] Z. X. Cui, S. Shen, J. Q. Yu, J. H. Si, D. P. Cai, Q. T. Wang, *Chem. Eng. J.* **2021**, *426*, 130068.
[45] L. Yin, Z. Xu, G. Yang, F. Guo, W. Guo, S. Zhao, S. Yang, *RSC Adv.* **2023**, *13*, 31667.
[46] D. Wang, J. Chen, W. Liang, G. Xue, J. Li, H. Jin, J. Wang, S. Wang, *Acs Appl. Energy Mater.* **2024**, *7*, 5792.
[47] Y. Liu, X. Zhang, J. Rong, D. Li, S. Lv, X. Sun, *J. Energy Storage* **2025**, *114*, 115886.
[48] H.-Y. Wang, H. Luo, M.-M. Liang, H. Ma, D. Lv, F. Qu, Y. Yin, Y. Zhou, X.-D. Zhang, H.-C. Zhao, Z.-C. Miao, *Rare Metals* **2025**, *44*, 4642.
[49] M. Liu, N. Deng, J. Ju, L. Fan, L. Wang, Z. Li, H. Zhao, G. Yang, W. Kang, J. Yan, B. Cheng, *Adv. Funct. Mater.* **2019**, *29*, 1905467.
[50] C. P. Li, M. Qiu, R. L. Li, X. Li, M. X. Wang, J. B. He, G. G. Lin, L. R. Xiao, Q. R. Qian, Q. H. Chen, J. X. Wu, X. Y. Li, Y. W. Mai, Y. M. Chen, *Adv. Fiber Mater.* **2022**, *4*, 43.
[51] Y. Zhang, V. Srot, I. Moudrakovski, Y. Feng, P. A. van Aken, J. Maier, Y. Yu, *Adv. Energy Mater.* **2019**, *9*, 1901470.
[52] X. Li, K. Li, S. Zhu, K. Fan, L. Lyu, H. Yao, Y. Li, J. Hu, H. Huang, Y.-W. Mai, J. B. Goodenough, *Angew. Chem. Int. Ed.* **2019**, *58*, 6239.
[53] J. Zhao, Z. Li, S. Lv, M. Wang, C. Li, X. Li, H. Chen, M. Li, X. Chen, F. Wang, W. Fan, J. Wu, Z. Wang, X. Li, Y. Chen, *InfoMat* **2023**, *5*, e12483.
[54] Q. Liu, J. Zhu, L. Zhang, Y. Qiu, *Renew. Sustain. Energy Rev.* **2018**, *81*, 1825.
[55] C. Li, M. Qiu, R. Li, X. Li, M. Wang, J. He, G. Lin, L. Xiao, Q. Qian, Q. Chen, J. Wu, X. Li, Y.-W. Mai, Y. Chen, *Adv. Fiber Mater.* **2022**, *4*, 43.
[56] H. Chen, M. Li, C. Li, X. Li, Y. Wu, X. Chen, J. Wu, X. Li, Y. Chen, *Chin. Chem. Lett.* **2022**, *33*, 141.
[57] Q. Jian, Y. Wan, J. Sun, M. Wu, T. Zhao, *J. Mater. Chem. A* **2020**, *8*, 20175.
[58] L. Yao, C. X. Hou, M. Q. Liu, H. B. Chen, Q. H. Zhao, Y. Zhao, Y. T. Wang, L. L. Liu, Z. W. Yin, J. M. Qiu, S. N. Li, R. Z. Qin, F. Pan, *Adv. Funct. Mater.* **2023**, *33*, 2209301.
[59] B. Zhang, F. Kang, J.-M. Tarascon, J.-K. Kim, *Prog. Mater. Sci.* **2016**, *76*, 319.
[60] S. Shi, Y. F. Si, Y. T. Han, T. Wu, M. I. Iqbal, B. Fei, R. K. Y. Li, J. L. Hu, J. P. Qu, *Adv. Mater.* **2022**, *34*, 2107938.
[61] Y. Q. Fu, Q. L. Wei, G. X. Zhang, X. M. Wang, J. H. Zhang, Y. F. Hu, D. N. Wang, L. C. Zuin, T. Zhou, Y. C. Wu, S. H. Sun, *Adv. Energy Mater.* **2018**, *8*, 1801445.
[62] H. Yu, Y. X. Zeng, N. W. Li, D. Y. Luan, L. Yu, X. W. Lou, *Sci. Adv.* **2022**, *8*, eabm5766.
[63] C.-L. Zhang, S.-H. Yu, *Chem. Soc. Rev.* **2014**, *43*, 4423.
[64] F. Shi, C. Chen, Z.-L. Xu, *Adv. Fiber Mater.* **2021**, *3*, 275.
[65] L. Hou, N. Wang, J. Wu, Z. Cui, L. Jiang, Y. Zhao, *Adv. Funct. Mater.* **2018**, *28*, 1801114.
[66] Y. Z. Zhou, F. D. Chen, H. Arandiyan, P. Y. Guan, Y. J. Liu, Y. Wang, C. Zhao, D. Y. Wang, D. W. Chu, *J. Energy Chem.* **2021**, *57*, 516.
[67] L. Qi, A. K. Khasraw, X. Jiawei, S. Zhihang, W. Yueyang, Z. Yajun, L. Mengyao, F. Yanchen, Z. Yi, S. Xiao-Ming, *Energy Mater.* **2024**, *4*, 400040.
[68] S. N. Yang, H. X. Du, Y. T. Li, X. S. Wu, B. S. Xiao, Z. X. He, Q. B. Zhang, X. W. Wu, *Green Energy Environ.* **2023**, *8*, 1531.
[69] V. Mathew, B. Sambandam, S. Kim, S. Kim, S. Park, S. Lee, M. H. Alfaruqi, V. Soundharrajan, S. Islam, D. Y. Putro, J. Y. Hwang, Y. K. Sun, J. Kim, *Acs Energy Lett.* **2020**, *5*, 2376.
[70] J. Xia, L. Liu, S. Jamil, J. J. Xie, H. X. Yan, Y. T. Yuan, Y. Zhang, S. Nie, J. Pan, X. Y. Wang, G. Z. Cao, *Energy Storage Mater.* **2019**, *17*, 1.
[71] J. W. Li, L. Zhang, W. L. Xin, M. Yang, H. L. Peng, Y. H. Geng, L. Yang, Z. C. Yan, Z. Q. Zhu, *Small* **2023**, *19*, 2304916.
[72] Y. Chen, D. Ma, S. Shen, P. Deng, Z. zhao, M. Yang, Y. Wang, H. Mi, P. Zhang, *Energy Storage Mater.* **2023**, *56*, 600.
[73] Y. Chen, D. Ma, K. Ouyang, M. Yang, S. Shen, Y. Wang, H. Mi, L. Sun, C. He, P. Zhang, *Nanomicro. Lett.* **2022**, *14*, 154.
[74] G. J. Li, L. Sun, S. L. Zhang, C. F. Zhang, H. Y. Jin, K. Davey, G. M. Liang, S. L. Liu, J. F. Mao, Z. P. Guo, *Adv. Funct. Mater.* **2024**, *34*, 2301291.
[75] Y. Guo, H. Jiang, B. Liu, X. Wang, Y. Zhang, J. Sun, J. Wang, *SmartMat* **2024**, *5*, e1231.
[76] A. I. Volkov, A. S. Sharlaev, O. Y. Berezina, E. G. Tolstopjatova, L. Fu, V. V. Kondratiev, *Mater. Lett.* **2022**, *308*, 131212.
[77] Y. Li, M. H. Chen, B. Liu, Y. Zhang, X. Q. Liang, X. H. Xia, *Adv. Energy Mater.* **2020**, *10*, 2000927.
[78] S. A. Liu, Z. Y. Cai, J. Zhou, A. Q. Pan, S. Q. Liang, *J. Mater. Chem. A* **2016**, *4*, 18278.
[79] X. T. Wu, C. S. Yin, M. F. Zhang, Y. Q. Xie, J. J. Hu, R. L. Long, X. M. Wu, X. W. Wu, *Chem. Eng. J.* **2023**, *452*, 139573.
[80] J. Wang, Z. Wang, J. Ni, L. Li, *Energy Storage Mater.* **2022**, *45*, 704.
[81] X. Liu, Z. Wang, Y. Niu, C. Liu, H. Chen, X. Ren, Z. Liu, W.-M. Lau, D. Zhou, *ACS Appl. Energy Mater.* **2022**, *5*, 3525.
[82] Y. M. Zhang, S. Y. Jiang, Y. L. Li, X. Z. Ren, P. X. Zhang, L. N. Sun, H. Y. Yang, *Adv. Energy Mater.* **2023**, *13*, 2202826.
[83] H. Wang, W. Hou, X. Wang, X. Xie, H. Peng, G. Ma, L. Zhu, Y. Xu, *Chem. Eur. J.* **2025**, *31*, e202403903.
[84] L. H. Zhang, X. Y. Qin, S. Q. Zhao, A. Wang, J. Luo, Z. L. Wang, F. Y. Kang, Z. Q. Lin, B. H. Li, *Adv. Mater.* **2020**, *32*, 1908445.
[85] C. Wang, G. H. Du, K. Ståhl, H. X. Huang, Y. J. Zhong, J. Z. Jiang, *J. Phys. Chem. C* **2012**, *116*, 4000.
[86] M. M. Han, J. W. Huang, S. Q. Liang, L. T. Shan, X. S. Xie, Z. Y. Yi, Y. R. Wang, S. Guo, J. Zhou, *iscience* **2020**, *23*, 100797.
[87] J. F. Zhang, Y. Zhao, Y. G. Zhang, J. D. Li, M. R. Babaa, N. Liu, Z. Bakenov, *Nanotechnology* **2020**, *31*, 095405.
[88] C. L. Teng, F. Yang, M. H. Sun, K. S. Yin, Q. T. Huang, G. Y. Fu, C. Q. Zhang, X. H. Lu, J. X. Jiang, *Chem. Sci.* **2019**, *10*, 7600.
[89] T. Xiong, Z. G. Yu, H. J. Wu, Y. H. Du, Q. D. Xie, J. S. Chen, Y. W. Zhang, S. J. Pennycook, W. S. V. Lee, J. M. Xue, *Adv. Energy Mater.* **2019**, *9*, 1803815.
[90] N. Zhang, F. Cheng, Y. Liu, Q. Zhao, K. Lei, C. Chen, X. Liu, J. Chen, *J. Am. Chem. Soc.* **2016**, *138*, 12894.
[91] G. Z. Fang, C. Y. Zhu, M. H. Chen, J. Zhou, B. Y. Tang, X. X. Cao, X. S. Zheng, A. Q. Pan, S. Q. Liang, *Adv. Funct. Mater.* **2019**, *29*, 1808375.
[92] H. Q. Song, C. F. Liu, C. K. Zhang, G. Z. Cao, *Nano Energy* **2016**, *22*, 1.
[93] L. N. Chen, Y. S. Ruan, G. B. Zhang, Q. L. Wei, Y. L. Jiang, T. F. Xiong, P. He, W. Yang, M. Y. Yan, Q. Y. An, L. Q. Mai, *Chem. Mater.* **2019**, *31*, 5342.
[94] Y. F. Song, L. Y. Jing, R. T. Wang, J. X. Cui, M. Li, Y. Q. Zhang, *J. Energy Chem.* **2024**, *89*, 599.
[95] K. X. Cai, S. H. Luo, J. Feng, J. C. Wang, Y. Zhan, Q. Wang, Y. H. Zhang, X. Liu, *Chem. Rec.* **2022**, *22*, e202100169.
[96] W. Jiang, H. Shi, X. Xu, J. Shen, Z. Xu, R. Hu, *Energy Environ. Mater.* **2021**, *4*, 603.
[97] Y. Cai, R. Chua, S. Z. Huang, H. Ren, M. Srinivasan, *Chem. Eng. J.* **2020**, *396*, 125221.
[98] S. Yang, M. Zhang, X. Wu, X. Wu, F. Zeng, Y. Li, S. Duan, D. Fan, Y. Yang, X. Wu, *J. Electroanal. Chem.* **2019**, *832*, 69.
[99] G. D. D. Sanglay, M. T. Castro, L. A. Limjuco, J. D. Ocon, *ChemElectroChem* **2025**, *12*, e202400714.
[100] C. Guo, R. Zhou, X. Liu, R. Tang, W. Xi, Y. Zhu, *Small* **2024**, *20*, 2306237.
[101] P. Yu, J. Zhou, M. Zheng, M. Li, H. Hu, Y. Xiao, Y. Liu, Y. Liang, *J. Colloid Interface Sci.* **2021**, *594*, 540.

© 2025 Wiley-VCH GmbH

25666223, 0, Downloaded from https://chemistry-europe.onlinelibrary.wiley.com/doi/10.1002/batt.202500655 by University of Ulsan, Wiley Online Library on [11/11/2025]. See the Terms and Conditions (https://onlinelibrary.wiley.com/terms-and-conditions) on Wiley Online Library for rules of use; OA articles are governed by the applicable Creative Commons License

[102] Y.-H. Zhao, S. Li, Y.-L. Huo, Z. Li, L.-L. Hou, Y.-Q. Wen, X.-X. Zhao, J.-J. Song, J.-C. Liu, *Rare Metals* **2025**, *44*, 2921.
[103] W. Chen, J. Feng, L. Yin, D. He, W. Gu, T. Wang, J. Liu, X. Zhao, C. Shi, J. Song, *Appl. Phys. Lett.* **2025**, *126*, 023901.
[104] L. Yin, C. Zhang, W. Chen, J. Xu, C. Shi, X. Qi, Y. Liu, J. Liu, S. Chen, X. Zhao, J. Song, *Chem. Eng. J.* **2025**, *512*, 162147.
[105] J.-C. Liu, L.-L. Ma, S. Li, L.-L. Hou, X.-R. Qi, Y.-Q. Wen, G.-P. Hu, N. Wang, Y. Zhao, X.-X. Zhao, *Rare Metals* **2023**, *42*, 3378.
[106] L. Ma, L.-J. Yu, J. Liu, Y.-Q. Su, S. Li, X. Zang, T. Meng, S. Zhang, J. Song, J. Wang, X. Zhao, Z. Cui, N. Wang, Y. Zhao, *Energy Storage Mater.* **2022**, *44*, 180.
[107] L. Ding, J. Gao, T. Yan, C. Cheng, L.-Y. Chang, N. Zhang, X. Feng, L. Zhang, *ACS Appl. Mater. Interfaces* **2022**, *14*, 17570.
[108] J. Wang, J.-G. Wang, H. Liu, Z. You, C. Wei, F. Kang, *J. Power Sources* **2019**, *438*, 226951.
[109] M. H. Chen, S. Xie, X. Y. Zhao, L. Peng, Y. Li, J. W. Zhang, M. S. Han, X. Q. Liang, Q. Liu, Y. Q. Zhang, Z. Chen, Q. G. Chen, *ACS Sustain. Chem. Eng.* **2022**, *10*, 12188.
[110] Y. L. He, Y. Pu, Y. Zheng, B. Zhu, P. Q. Guo, X. Y. Zhang, L. He, X. M. Wan, H. Tang, *J. Phys. Chem. Solids* **2024**, *184*, 111669.
[111] F. Tang, T. He, H. H. Zhang, X. W. Wu, Y. K. Li, F. N. Long, Y. H. Xiang, L. Zhu, J. H. Wu, X. M. Wu, *J. Electroanal. Chem.* **2020**, *873*, 114368.
[112] B. Jiang, C. Xu, C. Wu, L. Dong, J. Li, F. Kang, *Electrochim. Acta* **2017**, *229*, 422.
[113] J. Hao, J. Mou, J. Zhang, L. Dong, W. Liu, C. Xu, F. Kang, *Electrochim. Acta* **2018**, *259*, 170.
[114] C. Zhu, G. Fang, J. Zhou, J. Guo, Z. Wang, C. Wang, J. Li, Y. Tang, S. Liang, *J. Mater. Chem. A* **2018**, *6*, 9677.
[115] J. Huang, Z. Wang, M. Hou, X. Dong, Y. Liu, Y. Wang, Y. Xia, *Nat. Commun.* **2018**, *9*, 2906.
[116] G. Fang, C. Zhu, M. Chen, J. Zhou, B. Tang, X. Cao, X. Zheng, A. Pan, S. Liang, *Adv. Funct. Mater.* **2019**, *29*, 1808375.
[117] Y. Fang, X.-Y. Yu, X. W. Lou, *Angew. Chem. Int. Ed.* **2019**, *58*, 7744.
[118] Y. Xu, C. Wang, P. Niu, Z. Li, L. Wei, G. Yao, F. Zheng, Q. Chen, *J. Mater. Chem. A* **2021**, *9*, 16150.
[119] F. Li, Y.-L. Liu, G.-G. Wang, D. Yan, G.-Z. Li, H.-X. Zhao, H.-Y. Zhang, H.-Y. Yang, *J. Mater. Chem. A* **2021**, *9*, 9675.
[120] P. Zhang, M. He, S. Xu, X. Yan, *J. Mater. Chem. A* **2015**, *3*, 10811.
[121] J. Tan, T. Feng, S. Hu, Y. Liang, S. Zhang, Z. Xu, H. Zhou, M. Wu, *Appl. Surf. Sci.* **2022**, *604*, 154578.
[122] J. Yang, G. Yao, Z. Q. Li, Y. H. Zhang, L. Z. Wei, H. L. Niu, Q. W. Chen, F. C. Zheng, *Small* **2023**, *19*, 2205544.
[123] D. Guo, W. Q. Zhao, F. P. Pan, G. L. Liu, *Batteries Supercaps* **2022**, *5*, e202100380.
[124] W. Fu, Y. Hou, L. Zhang, T. Ma, G. Duan, S. Yang, *New J. Chem.* **2025**, *49*, 11254.
[125] J. Long, Z. Yang, F. Yang, J. Cuan, J. Wu, *Electrochim. Acta* **2020**, *344*, 136155.
[126] J. Wang, Z. Wang, Z. Liu, X. Meng, S. Wang, Z. Wang, *Ionics* **2024**, *30*, 3319.
[127] B. Li, Z. Nie, M. Vijayakumar, G. Li, J. Liu, V. Sprenkle, W. Wang, *Nat. Commun.* **2015**, *6*, 6303.
[128] Y. L. Wang, Q. L. Sun, Q. Q. Zhao, J. S. Cao, S. H. Ye, *Energy Environ. Sci.* **2011**, *4*, 3947.
[129] J. Zhang, Z. Xiong, X. S. Zhao, *J. Mater. Chem.* **2011**, *21*, 3634.
[130] C. Bai, H. Jin, Z. Gong, X. Liu, Z. Yuan, *Energy Storage Mater.* **2020**, *28*, 247.
[131] D. Gong, B. Wang, J. Zhu, R. Podila, A. M. Rao, X. Yu, Z. Xu, B. Lu, *Adv. Energy Mater.* **2017**, *7*, 1601885.
[132] H. Pan, B. Li, D. Mei, Z. Nie, Y. Shao, G. Li, X. S. Li, K. S. Han, K. T. Mueller, V. Sprenkle, J. Liu, *ACS Energy Lett.* **2017**, *2*, 2674.
[133] H. Tian, T. Gao, X. Li, X. Wang, C. Luo, X. Fan, C. Yang, L. Suo, Z. Ma, W. Han, C. Wang, *Nat. Commun.* **2017**, *8*, 14083.
[134] H. Yang, Y. Qiao, Z. Chang, H. Deng, P. He, H. Zhou, *Adv. Mater.* **2020**, *32*, 2004240.
[135] H. Tian, S. Zhang, Z. Meng, W. He, W.-Q. Han, *ACS Energy Lett.* **2017**, *2*, 1170.
[136] X. Zeng, X. Meng, W. Jiang, J. Liu, M. Ling, L. Yan, C. Liang, *ACS Sustain. Chem. Eng.* **2020**, *8*, 14280.
[137] Q. Zhang, Y.-H. Zeng, S.-H. Ye, S. Liu, *J. Power Sources* **2020**, *463*, 228212.
[138] S. Y. Ding, Q. W. Chen, S. Chen, Y. D. Tian, J. T. Zhang, *Chin. Chem. Lett.* **2023**, *34*, 108232.
[139] Y. Hu, Y. Chen, Y. Liu, W. Li, M. Zhu, P. Hu, H. Jin, Y. Li, *Micropor. Mesopor. Mater.* **2018**, *270*, 67.
[140] Z. Li, L. Yin, *Nanoscale* **2015**, *7*, 9597.
[141] S. Maiti, A. Pramanik, U. Manju, S. Mahanty, *ACS Appl. Mater. Interfaces* **2015**, *7*, 16357.
[142] H. Zhang, W. Zhao, M. Zou, Y. Wang, Y. Chen, L. Xu, H. Wu, A. Cao, *Adv. Energy Mater.* **2018**, *8*, 1800013.
[143] J. Wang, H. Sun, Y. Wu, H. Hu, F. Duan, M. Du, S. Lu, *ChemCatChem* **2025**, *17*, e01981.
[144] S. Baskaran, G. P. Mageswari, A. Muthukrishnan, *ChemCatChem* **2025**, *17*, e00598.
[145] Y. He, M. Liu, S. Chen, J. Zhang, *Sci. China Chem.* **2022**, *65*, 391.
[146] W. Shang, W. Yu, Y. Liu, R. Li, Y. Dai, C. Cheng, P. Tan, M. Ni, *Energy Storage Mater.* **2020**, *31*, 44.
[147] W. Zhou, D. Zhu, J. He, J. Li, H. Chen, Y. Chen, D. Chao, *Energy Environ. Sci.* **2020**, *13*, 4157.
[148] J. Liu, C. Guan, C. Zhou, Z. Fan, Q. Ke, G. Zhang, C. Liu, J. Wang, *Adv. Mater.* **2016**, *28*, 8732.
[149] S. Yang, C. Li, Y. Wang, S. Chen, M. Cui, X. Bai, C. Zhi, H. Li, *Energy Storage Mater.* **2020**, *33*, 230.
[150] X. Li, Y. Tang, J. Zhu, H. Lv, L. Zhao, W. Wang, C. Zhi, H. Li, *Small* **2020**, *16*, 2001935.
[151] X. J. Li, Y. C. Tang, H. M. Lv, W. L. Wang, F. N. Mo, G. J. Liang, C. Y. Zhi, H. F. Li, *Nanoscale* **2019**, *11*, 17992.
[152] J. Q. Yu, D. P. Cai, J. H. Si, H. B. Zhan, Q. T. Wang, *J. Mater.Chem. A* **2022**, *10*, 4100.
[153] T. Xu, M. Zhao, Z. Su, Z. Li, V. G. Pol, C.-T. Lo, *Energy Fuels* **2021**, *35*, 16194.
[154] L. L. Li, Y. C. Ma, F. Y. Cui, Y. Li, D. S. Yu, X. T. Lian, Y. X. Hu, H. Y. Li, S. J. Peng, *Adv. Mater.* **2023**, *35*, 2209628.
[155] J. Lin, C. Ji, G. Guo, Y. Luo, P. Huang, F. Xu, L. Sun, W. Pfleging, K. S. Novoselov, *Angew. Chem. Int. Ed.* **2025**, *64*, e202501721.
[156] A. Naveed, T. Rasheed, B. Raza, J. Chen, J. Yang, N. Yanna, J. Wang, *Energy Storage Mater.* **2022**, *44*, 206.
[157] C. Wang, X. Zhang, C. Li, N. Li, X. Xu, *Batteries Supercaps* **2025**, *8*, e202400706.
[158] W. Lu, Y. Shao, R. Yan, Y. Zhong, J. Ning, Y. Hu, *Batteries Supercaps* **2024**, *7*, e202300486.
[159] P. Yang, K. Zhang, S. Liu, W. Zhuang, Z. Shao, K. Zhu, L. Lin, G. Guo, W. Wang, Q. Zhang, Y. Yao, *Adv. Funct. Mater.* **2024**, *34*, 2410712.
[160] L. Yang, L. Meng, X. Ji, S. Cheng, *Batteries Supercaps* **2023**, *6*, e202300158.
[161] L. Wu, Y. Dong, *Energy Storage Mater.* **2021**, *41*, 715.
[162] Y. Zeng, X. Zhang, R. Qin, X. Liu, P. Fang, D. Zheng, Y. Tong, X. Lu, *Adv. Mater.* **2019**, *31*, 1903675.
[163] W. Dong, J.-L. Shi, T.-S. Wang, Y.-X. Yin, C.-R. Wang, Y.-G. Guo, *RSC Adv.* **2018**, *8*, 19157.
[164] S. H. Baek, Y. J. Cho, J. M. Park, P. Xiong, J. S. Yeon, H. H. Rana, J. H. Park, G. Jang, S. J. Lee, H. S. Park, *Int. J. Energy Res.* **2022**, *46*, 7201.
[165] J. Li, Q. Lin, Z. Zheng, L. Cao, W. Lv, Y. Chen, *ACS Appl. Mater. Interfaces* **2022**, *14*, 12323.
[166] Y. Wang, N. Li, H. Liu, J. Shi, Y. Li, X. Wu, Z. Wang, C. Huang, K. Chen, D. Zhang, T. Wu, P. Li, C. Liu, L. Mi, *Adv. Fiber Mater.* **2023**, *5*, 2002.
[167] J. Ye, T. Ge, X. Qu, M. M. Mohideen, C. Wang, P. Hu, Y. Liu, *Adv. Funct. Mater.* **2025**, *35*, 2425358.
[168] F. Xie, H. Li, X. Wang, X. Zhi, D. Chao, K. Davey, S.-Z. Qiao, *Adv. Energy Mater.* **2021**, *11*, 2003419.
[169] C. Li, Z. Sun, T. Yang, L. Yu, N. Wei, Z. Tian, J. Cai, J. Lv, Y. Shao, M. H. Rümmeli, J. Sun, Z. Liu, *Adv. Mater.* **2020**, *32*, 2003425.
[170] T. Liu, J. Hu, C. Li, Y. Wang, *Acs Appl. Energy Mater.* **2019**, *2*, 4379.
[171] B. X. Wang, J. Y. Hao, H. Xu, M. X. Sun, C. Wu, W. Qin, X. Q. Wu, Q. L. Wei, *ACS Appl. Mater. Interfaces* **2024**, *16*, 46879.
[172] P. Xue, C. Guo, N. Wang, K. Zhu, S. Jing, S. Kong, X. Zhang, L. Li, H. Li, Y. Feng, W. Gong, Q. Li, *Adv. Funct. Mater.* **2021**, *31*, 2106417.
[173] R. Zhu, X. Ren, L. Wu, L. Tian, H. Zhang, Y. Meng, J. Zhou, *Adv. Mater.* **2025**, *37*, 2503516.
[174] S. Yang, Y. Li, H. Du, Y. Liu, Y. Xiang, L. Xiong, X. Wu, X. Wu, *ACS Sustain. Chem. Eng.* **2022**, *10*, 12630.
[175] S. Rao, W. Song, Z. Lu, Q. Ma, L. Ye, M. Fujishige, K. Takeuchi, M. Endo, J. Niu, F. Wang, *Nano Res.* **2025**, *18*, 94907588.
[176] X. Li, Q. Li, Y. Hou, Q. Yang, Z. Chen, Z. Huang, G. Liang, Y. Zhao, L. Ma, M. Li, Q. Huang, C. Zhi, *ACS Nano* **2021**, *15*, 14631.
[177] E. Pargoletti, Y. Gogotsi, *ChemCatChem* **2025**, *17*, e00730.
[178] L. Sha, J.-Y. Qu, B.-B. Sui, P.-F. Wang, Z. Gong, Y.-H. Zhang, Y.-H. Wu, L.-N. Zhao, J.-J. Tang, F.-N. Shi, *Solid State Ion.* **2024**, *406*, 116472.

© 2025 Wiley-VCH GmbH

25666223, 0, Downloaded from https://chemistry-europe.onlinelibrary.wiley.com/doi/10.1002/batt.202500655 by University of Ulsan, Wiley Online Library on [11/11/2025]. See the Terms and Conditions (https://onlinelibrary.wiley.com/terms-and-conditions) on Wiley Online Library for rules of use; OA articles are governed by the applicable Creative Commons License

[179] G. Li, Z. Liu, Q. Huang, Y. Gao, M. Regula, D. Wang, L.-Q. Chen, D. Wang, *Nat. Energy* **2018**, *3*, 1076.
[180] L. Sha, B.-B. Sui, P.-F. Wang, Z. Gong, Y.-H. Zhang, Y.-H. Wu, L.-N. Zhao, J.-J. Tang, F.-N. Shi, *Chem. Eng. J.* **2024**, *481*, 148393.
[181] Y. Zong, H. He, Y. Wang, M. Wu, X. Ren, Z. Bai, N. Wang, X. Ning, S. X. Dou, *Adv. Energy Mater.* **2023**, *13*, 2300403.
[182] Q. Ni, B. Kim, C. Wu, K. Kang, *Adv. Mater.* **2022**, *34*, 2108206.
[183] A. O'Donoghue, M. Shine, I. M. Povey, J. F. Rohan, *Batteries Supercaps* **2024**, *7*, e202300447.
[184] C. A. Heck, T. Scharmann, M. Osenberg, A. Diener, I. Manke, P. Michalowski, A. Kwade, *Batteries Supercaps* **2024**, *7*, e202300487.
[185] Z. Li, Z. Lu, T. Zhang, B. Qin, W. Yan, L. Dong, J. Dong, C. Ma, Z. Chen, W. Li, Y. Zheng, J. Zhang, *Batteries Supercaps* **2024**, *7*, e202400435.
[186] F. H. Wu, B. K. Wu, Y. B. Mu, L. F. Zou, J. F. He, M. Yang, L. Zeng, *J. Power Sources* **2024**, *597*, 234177.
[187] L. Cheng, W. Li, M. Li, S. Zhou, J. Yang, W. Ren, L. Chen, Y. Huang, S. Yu, J. Wei, *Adv. Funct. Mater.* **2024**, *34*, 2408863.
[188] R.-h. Li, B.-b. Sui, P.-f. Wang, Z. Gong, Y.-h. Wu, Y.-h. Zhang, L.-n. Zhao, J.-j. Tang, F.-n. Shi, *J. Alloys Compd.* **2024**, *997*, 174899.
[189] P. Wang, B. Niu, H. Chen, X. Wang, *Small Methods* **2025**, *9*, e01055.
[190] A. Hussain, M. M. Mohamed, M. Faheem, Y. P. Hardianto, M. O. Aijaz, M. R. Karim, M. A. Aziz, *J. Polym. Sci.* **2025**, *63*, 3824.
[191] Z. Wang, T. Guo, M. Zhang, L. Zhao, T. He, *J. Energy Storage* **2025**, *108*, 115154.

Manuscript received: August 24, 2025
Revised manuscript received: September 21, 2025
Version of record online:

© 2025 Wiley-VCH GmbH

25666223, 0, Downloaded from https://chemistry-europe.onlinelibrary.wiley.com/doi/10.1002/batt.202500655 by University of Ulsan, Wiley Online Library on [11/11/2025]. See the Terms and Conditions (https://onlinelibrary.wiley.com/terms-and-conditions) on Wiley Online Library for rules of use; OA articles are governed by the applicable Creative Commons License